Title

The Intra-Host Evolutionary Landscape And Pathoadaptation Of Persistent *Staphylococcus aureus* In Chronic Rhinosinusitis

Authors

Ghais Houtak[1,2†], George Bouras[1,2†], Roshan Nepal[1,2], Gohar Shaghayegh[1,2], Clare Cooksley[1,2], Alkis James Psaltis[1,2], Peter-John Wormald[1,2], Sarah Vreugde[1,2*]

Author's institutional affiliations

[1] Adelaide Medical School, Faculty of Health and Medical Sciences, The University of Adelaide, Adelaide, Australia.

[2] The Department of Surgery - Otolaryngology Head and Neck Surgery, University of Adelaide and the Basil Hetzel Institute for Translational Health Research, Central Adelaide Local Health Network, South Australia, Australia

[†] These authors contributed equally.

[*] Correspondence: sarah.vreugde@adelaide.edu.au; Tel: +618-8222-7158

Conflicts of interest

The authors state that the study was conducted without any commercial and financial relationship that could be interpreted as a potential conflict of interest.

Abstract

Chronic rhinosinusitis (CRS) is a common chronic sinonasal mucosal inflammation associated with *Staphylococcus aureus* biofilm and relapsing infections. This study aimed to determine rates of *S. aureus* persistence and pathoadaptation in CRS patients by investigating the genomic relatedness and antibiotic resistance/tolerance in longitudinally collected *S. aureus* clinical isolates.

A total of 68 *S. aureus* isolates were sourced from 34 CRS patients at least six months apart. Isolates were grown into 48-hour biofilms and tested for tolerance to antibiotics. A hybrid sequencing strategy was used to obtain high-quality reference-grade assemblies of all isolates. Single nucleotide variants (SNV) divergence in the core genome and sequence type clustering were used to analyse the relatedness of the isolate pairs. Single nucleotide and structural genome variations, plasmid similarity, and plasmid copy numbers between pairs were examined.

Our analysis revealed that 41% (14/34 pairs) of *S. aureus* isolates were persisters, while 59% (20/34 pairs) were non-persisters. Persister isolates showed episode-specific mutational changes over time with a bias towards events in genes involved in adhesion to the host and mobile genetic elements such as plasmids, prophages, and insertion sequences. A significant increase in the copy number of conserved plasmids of persister strains ($p<0.05$) was seen, indicating a role of the "mobilome" in promoting persistence. This was accompanied by a significant increase in biofilm tolerance against all tested antibiotics ($p<0.001$), which was linked to a significant increase in biofilm biomass ($p<0.05$) over time, indicating a biofilm central pathoadaptive process in persisters.

In conclusion, our study provides important insights into the mutational changes underlying *S. aureus* persistence in CRS patients highlighting pathoadaptive mechanisms

42 in *S. aureus* persisters culminating in increased biofilm biomass linked to an increase in

43 plasmid copy number over time.

Abbreviations

AERD, aspirin-exacerbated respiratory disease

AMR, Antimicrobial Resistance

CARD, Comprehensive Antibiotic Resistance Database

CDS, coding sequences

CFU, Colony Forming Unit

CI, Clinical Isolate

CLSI, Clinical and Laboratory Standards Institute

CRS, Chronic Rhinosinusitis

CRSsNP, CRS without Nasal Polyposis

CRSwNP, CRS with Nasal Polyposis

CV, Crystal Violet

MFU, McFarland Units

MIC, Minimum Inhibitory Concentration

MIC50, MIC required to inhibit the growth of 50% of organisms

MIC90, MIC required to inhibit the growth of 90% of organisms

MLST, Multi-Locus Sequence Typing

NCTC, National Collection of Type Culture

NGS, Next Generation Sequencing

ONT, Oxford nanopore technology

PCR, Polymerase Chain Reaction

SNV, Single-Nucleotide Variant

SV, structural variants

VFDB, Virulence Factor Database

68 VLKCs, Variable-length k-mer clusters

69 WGS, Whole Genome Sequencing

Introduction

Chronic rhinosinusitis (CRS) is characterised by ongoing inflammation of the paranasal sinuses and nasal mucosal lining, which causes symptoms such as nasal congestion, diminished sense of smell, facial pain, and breathing difficulties (Fokkens et al., 2020). Around 10% of people worldwide suffer from CRS, making it a common condition (Hastan et al., 2011).

CRS is clinically subdivided based on its phenotype into two subcategories, CRS with nasal polyps (CRSwNP) and CRS without nasal polyps (CRSsNP) (Hopkins, 2019). Although the pathogenesis of CRS remains unknown, it is known to be a heterogeneous multi-factorial chronic inflammatory disease that frequently co-occurs with conditions such as ciliary dysfunction, aspirin-exacerbated respiratory disease (AERD), and asthma (Fokkens et al., 2020).

It is thought that microbes impact the pathophysiology of CRS. One of the bacteria most abundantly found in the sinuses of CRS patients is *Staphylococcus aureus*, which is frequently associated with exacerbations of the condition (Okifo, Ray, & Gudis, 2022; Vickery, Ramakrishnan, & Suh, 2019).

Several mechanisms of involvement of *S. aureus* in the pathophysiology of CRS have been proposed, including *S. aureus* biofilms as a modulator of chronic mucosal inflammation and relapsing infections (Hoggard et al., 2017; Vickery et al., 2019). Moreover, *S. aureus* mucosal biofilms are associated with poor post-surgical outcomes (Psaltis, Weitzel, Ha, & Wormald, 2008; Singhal, Foreman, Jervis-Bardy, & Wormald, 2011).

Despite the lack of high-level evidence for the effectiveness of antibiotics in treating CRS and its exacerbations, they are commonly prescribed to CRS patients (Barshak &

Durand, 2017; Fokkens et al., 2020). Moreover, antibiotics are often ineffective at eliminating the biofilm nidus resulting in a relapsing course of infectious exacerbations (C. W. Hall & Mah, 2017).

Previously we have shown with pulsed-field gel electrophoresis that subjects suffering from CRS are colonised with identical pulsotype *S. aureus* strains months apart in 79% of cases despite multiple courses of systemic antibiotics (Drilling et al., 2014). This suggests that the bacteria can persist in the sinuses despite antibiotic treatment. However, what is less clear is the pathogenic adaptation and phenotypic changes that occur during chronic infection of difficult-to-treat CRS patients.

This study aimed to evaluate the intra-host relatedness of longitudinal *S. aureus* clinical isolates (CI) collected from the nasal cavities of subjects suffering from CRS and characterise the adaption that enables persistence in the host using hybrid long and short read assembled reference-level genomes. Furthermore, intra- and inter-host variability in *S. aureus* phenotype regarding antimicrobial resistance and biofilm tolerance to antibiotics was evaluated to identify phenotypic pathoadaptation of persistent strains.

Materials and Methods

Ethics

This project was approved by the Central Adelaide Local Health Network Human Research Ethics Committee under the following reference number: HREC/15/TQEH/132.

Clinical isolate retrieval

S. aureus CIs were retrieved from a bacterial biobank comprised of samples stored in 25% glycerol stock at −80 °C, obtained from swabs taken from the sinonasal cavity of subjects. The swabs were collected from ear-nose-throat inpatient clinic follow-ups and during sinonasal surgery. To be included in this study, longitudinal CI pairs had to be isolated from swabs obtained from patients who fulfilled the EPOS 2020 criteria for difficult-to-treat CRS (Fokkens et al., 2020). The diagnostic criteria and retrieval of asthma, aspirin sensitivity and CRS subtype are elaborated in supplementary text ST1. Only clinical isolate pairs with a time difference of over five months between collections were included in the study. When a subject had more than two clinical isolates available at different timepoints, the isolated pair with the largest time difference was selected. We termed the first recovered isolate group T0, whereas the isolates recovered at later timepoints were termed T1. For all experiments, the clinical isolates were grown overnight on nutrient agar plates (Thermo Fisher Scientific, CM0003, Waltham, USA) from glycerol stock at 37°C unless otherwise specified.

Antibiotic exposure

The antibiotic exposure of subjects was assessed based on the antibiotic scripts in their medical records. All antibiotic treatments prescribed to the subjects between their first and second sample collection were extracted. The total antibiotic exposure was calculated as the cumulative number of days prescribed for the treatments (Schechner, Temkin, Harbarth, Carmeli, & Schwaber, 2013).

Genomic DNA extraction and sequencing

For all clinical isolates, hybrid long and short sequencing was performed. The genomic DNA of the *S. aureus* clinical isolates was extracted using the DNeasy Blood & Tissue Kit (Qiagen, 69504, Hilden, Germany) following the manufacturer's guidelines. The extracted DNA was sequenced using the Oxford nanopore technology (ONT) on the MinION Mk1C (Oxford Nanopore Technologies, Oxford, UK) for long-read sequencing. The Rapid Barcoding Kit (Oxford Nanopore Technology, SQK-RBK 110.96) was used to sequence the long-read *S. aureus* whole genome on R9.4.1 MinION flowcells (Oxford Nanopore Technology), using 50 ng of the isolated DNA. Base-calling was conducted with Guppy v 6.2.11 in super accuracy mode, using the 'dna_r9.4.1_450bps_sup.cfg' configuration (Oxford Nanopore Technology). The short-read sequencing was done at a commercial sequencing facility (SA Pathology, Adelaide, SA, Australia) as previously described by Shaghayegh et al. (Shaghayegh et al., 2023). Short-read sequencing was carried out on the Illumina platform, using the Illumina NextSeq 550 (Illumina Inc, San Diego, USA) and NextSeq 500/550 Mid-Output kit v2.5 (Illumina Inc., FC-131-1024). To prepare for short-read sequencing, the genomic DNA was isolated using the NucleoSpin Microbial DNA kit (Machery-Nagel GmbH and Co.KG, 740235.50, Duren, Germany). The

sequencing libraries were prepared using a modified protocol for the Nextera XT DNA library preparation kit (Illumina Inc. FC-131-1024). The genomic DNA was fragmented, after which a low-cycle PCR reaction was used to amplify the Nextera XT indices to the DNA fragments. One hundred fifty bp reads were obtained by sequencing after manual purification and normalisation of the amplicon library.

Bioinformatics

Chromosome assembly: We created complete chromosomal assemblies of *S. aureus* using the custom Snakemake pipeline (Molder et al., 2021) that can be accessed via https://github.com/gbouras13/hybracter and a Snaketool (Roach et al., 2022) powered command line tool called hybracter (Bouras, hybracter). Briefly, the long reads were reduced to 250 Mbp for each sample using Rasusa (M. Hall, 2022). Adapters and barcodes were removed using Porechop (Ryan R. Wick, Porechop), short reads were filtered and trimmed with low-quality regions, and adapters were removed using fastp (Chen, Zhou, Chen, & Gu, 2018). Long-read-only assemblies were created using Flye v2.9.1 with the option "--nano-hq." (Kolmogorov, Yuan, Lin, & Pevzner, 2019). Assemblies, including contigs with a length greater than 2.5 Mb, were kept and denoted as the putative chromosomal. The resulting chromosomes were first polished with long reads using Medaka v1.7.0 (ONT, 2022), then with short reads using Polypolish v0.5.0. (R. R. Wick & Holt, 2022) . After the first round of polishing, the chromosomes were reoriented to start at the *dnaA* gene using the python program called dnaapler (Bouras, dnaapler). Finally, chromosomes were polished for a second time using Polypolish and then with POLCA (Zimin & Salzberg, 2020).

Plasmid assembly: Plassembler v 0.1.4 (Bouras, Plassembler) was used to assemble bacterial plasmids from a combination of long and short sequencing reads. Firstly, the

177 short reads are filtered using fastp. The long reads were filtered using nanoFilt (De
178 Coster, D'Hert, Schultz, Cruts, & Van Broeckhoven, 2018) and then assembled using Flye.
179 The largest contig was evaluated to see if the assembly contained more than one contig.
180 If this contig was over 90% of the length of the chromosome size (~2.5 MB), it was
181 identified as the chromosome. All other contigs were deemed putative plasmid contigs.
182 Both long and short reads were then mapped twice, first to the chromosome and then to
183 the plasmid contigs. For the mapping, minimap2 (H. Li, 2018) was used for the long
184 reads, while BWA-MEM (Heng Li, 2013) was used for the short reads. Reads aligned to
185 the plasmid contigs or not aligned to the chromosome were extracted, combined, and
186 de-duplicated. To produce the final plasmid contigs, these reads were assembled using
187 Unicycler v0.5.0 (R. R. Wick, Judd, Gorrie, & Holt, 2017).
188 Annotation: Chromosome and plasmid assemblies were annotated with Bakta v1.5.0
189 (Schwengers et al., 2021). The assemblies were typed according to multi-locus sequence
190 typing (MLST) using the program MLST (Seemann, mlst) and assigned to clonal
191 complexes of PubMLST (Jolley, Bray, & Maiden, 2018). Variable-length-k-mer clusters
192 (VLKCs) were used to query the assemblies with k-mer lengths ranging from 13 to 28
193 and a sketch size of 9984 using the pp-sketchlib tool (Lees et al., 2019). The VLKCs were
194 assigned to the pre-built PopPUNK Staphopia database of 103 clusters for phylogenetic
195 analysis (Petit & Read, 2018). The phylogenetic tree was visualised using the ggtree R
196 package (Xu et al., 2022).
197 Chromosome analysis: The presence or absence of resistance and virulence genes in the
198 genome of the CIs was determined by screening contigs using ABRicate v1.0.1
199 (Seemann, Abricate) against the Comprehensive Antibiotic Resistance Database (CRAD)
200 (Jia et al., 2017) and the Virulence Factor Database (VFDB) (Liu, Zheng, Jin, Chen, &
201 Yang, 2019).

Genome-wide association analysis was done by first creating a pangenome of the 34 T0 isolates with panaroo v1.3.2 (Tonkin-Hill et al., 2020) and then testing the significance of each gene with Scoary v1.6.16 using default parameters (Brynildsrud, Bohlin, Scheffer, & Eldholm, 2016). All following paired *S. aureus* genomic analysis was conducted using a Snakemake pipeline. Firstly, small variants, such as single nucleotide variants (SNVs) and small insertions and deletions, were called using Snippy v 4.6.0. (Seemann, 2015), with the raw FASTQ short reads from the Timepoint T1 isolates were compared against the corresponding GenBank file of the assembled Timepoint T0 isolate for each CIs pair. All larger structural differences were called using two methods: Nucdiff v2.0.3 (Khelik, Lagesen, Sandve, Rognes, & Nederbragt, 2017) and Sniffles v2.0.7 (Sedlazeck et al., 2018). For Nucdiff, chromosome assembly of the T0 isolate was compared against the corresponding T1 isolate. For, Sniffles, all T1 isolate long reads were first aligned to the T0 isolate genome using minimap2 v 2.24 (H. Li, 2018) specifying '-ax map-ont' parameters. The resulting BAM was used as input for Sniffles.

The large structural variant CIs pairs of subject 420 and 4875 were manually annotated by mapping all timepoint T1 long reads to the T0 assembly using minimap2 v 2.24 specifying '-ax map-ont', followed by sorting the resulting BAM file using samtools (Danecek et al., 2021). Structural deletions were visualised in R using the gggenomes, and the long-read pile-up was visualised using the Gviz packages (Ankenbrand, 2022; Hahne & Ivanek, 2016).

Plasmid analysis: For each putative plasmid contig derived from the output of Plassembler, Mobtyper v1.4.9 (Robertson & Nash, 2018) was run to determine each plasmid's predicted mobility and replicon marker. The minhash ('Mash') distance was calculated between each pair of plasmids using mash v2.3 (Ondov et al., 2016). A plasmid pangenome was created using panaroo v1.3.2. To determine shared plasmid

genes using the `gene_presence_absence. Rtab' output, the Jaccard index based on gene presence and absence, was calculated between each plasmid pair. Following the analysis by Hawkey et al., plasmids were empirically determined to be the same plasmid using thresholds of Mash similarity > 0.98 and Jaccard index > 0.7 (Hawkey et al., 2022). Additionally, plasmids were determined to be beta-lactamase-carrying if they carried the *blaZ*, *blaI* and *blaR1* gene operon. All plasmid-copy numbers were obtained using Plassembler v0.1.4.

Relatedness of isolate pairs

A two-step approach was used to classify isolate pairs as either closely related 'same strain' or not closely related 'different strain'. Firstly, the Sequence Types obtained from MLST and clusters generated by PopPUNK were compared between each isolate pair. If either of these metrics differed in the CI pair, they were considered to belong to different strains. The second step involved analysing the number of small variants outputted by Snippy. Isolate pairs with 100 or fewer single nucleotide variants (SNVs) between the first and second timepoint were classified as the same strain.

Planktonic Antibiotic Susceptibility

Susceptibility testing followed Clinical and Laboratory Standards Institute (CLSI) guidelines (CLSI, 2020). Seven antibiotics were chosen for susceptibility testing according to their common use in medical practice. These were: amoxicillin in combination with clavulanic acid (augmentin), clarithromycin, clindamycin, doxycycline, erythromycin, gentamicin, and mupirocin (Sigma-Aldrich, St. Louis, USA). Minimum Inhibitory Concentrations (MICs) were obtained for the planktonic form of all isolates, utilising the microbroth dilution assay (Wiegand, Hilpert, & Hancock, 2008). The

antibiotics were tested at 0.06–32 mg/L dilution range. The assay was repeated at least twice per CI. The MIC50, MIC90 and antibiotic non-susceptibility proportions were calculated adopting the susceptibility breakpoints published by the CLSI.

Biofilm Antibiotic Tolerance

The biofilm tolerance assay was based on a 96-well plate adapting the procedures used by Mah et al. (Mah, 2014). Each isolate was exposed to the same antibiotics used for the planktonic antibiotic susceptibility testing. The concentrations ranged from 1.25–640 mg/L. In brief, the CIs were cultured on Mueller-Hinton agar (Sigma-Aldrich). Then, single colonies of *S. aureus* were suspended in 0.9 % saline to a turbidity reading of 0.5 McFarland Units (MFU). The 0.5 MFU bacterial suspension was diluted 100-fold in Mueller-Hinton broth to achieve a 5×10^5 CFU/ml before inoculation in a 96-well plate (200 µL). Plates underwent a 48-hour incubation at 37°C with sheer force on a rotating plate set at 70 rpm (3D Gyratory Mixer, Ratek Instruments, Australia). Following the incubation, the supernatants were gently aspirated with a minimum agitation of the biofilms. These biofilms were then exposed to different antibiotics in serial diluted (200 µL) Mueller-Hinton broth for 24 hours. After incubation with antibiotics, the supernatants were aspirated gently, and non-adherent planktonic bacteria were removed by gently washing with sterile phosphate-buffered saline (PBS). Subsequently, the biofilm tolerance was assayed using a resazurin viability method, alamarBlue Cell Viability Reagent (Thermo Fisher Scientific, DAL1025), as per the manufacturer's instruction (Pettit et al., 2005). The assay was repeated twice per CI with two replicates.

Biofilm Biomass Assay

To quantify the total biofilm biomass, the Crystal Violet (CV) staining assay was used (Stiefel et al., 2016). Inoculated 96-well plates underwent a 48-hour incubation at 37°C on a rotating plate set at 70 rpm to induce biofilm formations. Following the incubation, the planktonic cells were removed by gently aspirating the supernatants and washing the wells twice with PBS. Subsequently, 200 µL of 0.1 % CV (Sigma-Aldrich, C6158) solution was added for 15 minutes. After washing the wells three times with sterile water and air-drying, the fixed CV was solubilised by adding 200 µL 30% acetic acid and shaking for one hour at room temperature. The absorbance was obtained at 595 nm with a FLUOstar Omega microplate reader (BMG Labtech, Ortenberg, Germany). The assay was repeated twice per strain, with six technical replicates.

Statistics

We used a generalised linear mixed model (GLMM) to analyse the antibiotic tolerance data. To assess the significance of each variable, a backwards stepwise regression approach using the log-likelihood ratio test was used to remove insignificant variables. The threshold of significance was set at a p-value<0.05. All analysis was performed with R v4.2.0. (R Core Team, 2017).

Data availability

The assembled chromosomes and plasmids, raw short and raw long read FASTQs, are accessible on the Sequence Read Archive (SRA) under the project code: PRJNA914892. The complete list of biosample accession numbers for each sample can be found in supplementary table 1.

Code Availability

All code used to generate all analyses & figures used in this manuscript can be found at https://github.com/gbouras13/CRS_Saureus_Evolutionary_Landscape.

Results

Clinical characteristics

Thirty-four *S. aureus* sequential pairs (68 clinical isolates from which 34 first timepoint (T0) and 34 second (T1) isolates) were included in this study, isolated from 34 subjects. The mean time between paired *S. aureus* CI collection was 18 months (range 6-52). Most subjects were classified as CRSwNP (85%) and having asthma (56%). The clinical characteristics of the subjects are summarised in Table S2.

S. aureus strains persist within the sinonasal cavities in 41% of cases

The MLST analysis revealed a total of seven clonal complexes (CCs), including CC1 (n=5, 7.3%), CC5 (n=4, 5.8%), CC8 (n=2, 2.9%), CC15 (n=5, 7.3%), CC22 (n=5, 7.3%), CC30 (n=9, 13.2%), and CC45 (n=14, 20.5%). A total of 24/68 CIs (35.2%) were not assigned to any CC (Fig. 1A). The analysis of the PopPUNK variable-length-k-mer clusters (VLKCs) identified a total of 16 clusters. Of the 34 isolate pairs, 18 (52.9%) pairs belonged to different CCs or VLKCs, indicating that they were not closely related isolates and were classified as 'different strain' pairs.

The relatedness was investigated for the 16 remaining pairs by analysing the number of SNVs in shared genes. The variants ranged from 2-2123, with 14/16 pairs having 69 or fewer SNVs and 2/16 pairs having more than 100 SNVs. Figure 1B shows the multimodal distribution of SNVs between all CI pairs and reflects the classification of pairs into different and same strain groupings. The two pairs with the same CC and VLKC groups and more than 100 SNVs divergence (host 4784, 846 SNVs; host 5911,

2123 SNVs) were classified as 'different strain' pairs due to the large number of SNVs and structural variations between pairs. Namely, the CI pair from host 4784 had 100 structural variations between T0 and T1 according to Sniffles, with the addition of a plasmid in the T1 isolate. Similarly, the CI pair from host 5911 had 143 structural variations between them. Accordingly, 14/34 pairs (41%) were classified as unambiguously in the 'same strain' group of persistent isolates, whilst 20/34 pairs (59%) were classified as being part of the 'different strain' group, where the subject had been colonised or infected by a different strain over time (Table S3). No genomic clustering was observed based on the order of CI collection of the pairs and the host's CRS phenotype or asthma status (Fig. 1A).

Chromosomally encoded antimicrobial resistance genes and virulence factors are widespread in *S. aureus* sinonasal isolates

Chromosomally encoded antimicrobial resistance (AMR) genes in the *S. aureus* isolates were assessed using the CARD database, revealing a range of 8-21 genes AMR per isolate. Most isolates (67/68) contained 8-13 AMR genes, including *arlR*, *arLR*, *arlS*, *lmrS*, *mepA*, *mepR*, *mgrA*, *norA* and *tet(38),* which were identified in all CIs (Fig. S1). Only one isolate (Host:2911, CI: C295) contained more than 13 AMR genes. Among the 40 CIs classified as being different strain pairs, the *blaZ* beta-lactamase gene was present in 22 of them. Notably, the prevalence of chromosomal *blaZ*-positive isolates increased from 9/20 (45%) in the first timepoint different strain group to 13/20 (65%) in the second timepoint different strain group, indicating a potential selective pressure for beta-lactamase-resistant isolates in the population. Remarkably, none of the isolates in the second timepoint of the different strain group contained the *ermC* gene, whereas, in the first timepoint, three isolates were found to carry multiple copies.

In the same strain group isolates, 11/28 (39.2%) were positive for a chromosomally encoded *BlaZ* beta-lactamase gene. Only one of the same strain pairs gained a chromosomally encoded *BlaZ* gene at the second timepoint (Fig. S1).

The presence of chromosomally encoded virulence factor genes in the *S. aureus* isolates was assessed using the VFDB database, revealing a range of 45-72 (median 57) genes per isolate (Fig. S2). Notably, all CIs contained the serine protease operon sspABC, also known as V8 protease, which has been previously associated with allergic sensitisation to *S. aureus* (Krysko, Teufelberger, Van Nevel, Krysko, & Bachert, 2019). Additionally, all isolates had immune evasion-associated factors such as the immunoglobulin-binding protein *sbi*, *adsA*, *lip*, *hly/hla*, *hlgAB*, *hld*, and *geh*. The *isdABCDEFG* operon was present in 67 out of 68 isolates. The *icaABCD* operon, associated with biofilm production, was present in all isolates, but interestingly, two isolates lacked the *icaR* (repressor) gene. Moreover, 61 and 66 isolates contained the *sak* and *scn* virulence factors, respectively, which are prophage encoded (Nepal et al., 2021). Notably, the prevalence of immune evasion factors *chp* (9/20 vs. 18/20) and *sdrE* (9/20 vs. 15/20) increased in the second timepoint different strain group. In contrast, the carriage of *sdrC* (13/20 vs. 7/20) decreased in the second timepoint of different strain group (Fig. S2). No remarkable alterations were observed in the acquisition or loss of virulence factors between the initial and subsequent timepoints of the same strain group.

Analysis of gene content in *S. aureus* isolates suggests a reduced virulence profile for incoming isolates

To investigate whether gene presence or absence was linked to persistence, a microbial gene presence-absence analysis was performed on the 34 Timepoint T0 isolates using Scoary. No statistically significant differences in gene content were found between the same and different strain isolates at T0 (BH p.adj > 0.05). However, the *chp* gene, involved in chemotaxis inhibition, was less prevalent in the persister same strain group (8/14 same strain vs. 18/20 different strain).

A subsequent microbial gene presence-absence analysis was conducted on the 40 different strain isolates to examine whether the gene content of the second timepoint T1 isolates differed from that of the T0 isolates. Although no statistically significant differences were observed, there was a clear trend for incoming T1 isolates to have fewer virulence factors than the T0 isolates they replaced, such as staphylococcal enterotoxins M, U, I, N, and G (present in 8/20 T1 isolates compared to 18/20 T0 isolates) and *chp* (9/20 T1 vs 18/20 T0 isolates).

Same strain SNV prevalence reveals heterogeneous host adaption

222 SNVs were observed across the 14 same-strain isolates, ranging from 2-69 per isolate. 8/14 pairs had less than 10 SNVs. Of these 222 SNVs, 148 were in putative coding sequences (CDS), 44 were synonymous SNPs, 3 were in-frame variants, 9 were frameshift variants, 4 were stop-gained variants, and the remaining 88 were missense-SNVs. Only three genes contained SNVs in more than one isolate, namely the ribosomal protein *rpsJ,* the transcription termination factor *clpC*, and the protease ATP-binding subunit *clpX*. Interestingly, MSCRAMM genes commonly harboured SNVs across the same strain pairs, with 11 SNVs occurring in 9 distinct MSCRAMM genes in 6 distinct

isolates, of which 6/11 mutations were synonymous. These include variants in the *sdrC* adhesin, fibronectin-binding proteins A and B (*fnbA* and *fnbB*), surface protein G (*sasG*) and iron-regulated surface-determining proteins *isdD*, *isdE* and *isdF*. Other adhesion genes, including Staphylocoagulase *coa*, extracellular adherence protein *eap*/map, and the extracellular matrix binding protein *EbhA* also had SNVs across isolates.

Structural variants in same strain CI pairs involve prophages, insertion sequences, MSCRAMM and AMR Genes & are not correlated with the number of SNVs

We detected a total of 37 structural variants (SV) among the 14 same strain isolates, ranging in size from small collapsed duplications (<10bp) to the acquisition of a 43793 bp *hlb*-disrupting Sa3int prophage in a single isolate pair. Only 10 SV were larger than 100bp, and all were found in 4/14 CI pairs, with one strain having 5 SV> 100bp. Notably, no relationship was observed between the number of SNVs and structural variations. The CI pair from host 5562, which had the second-lowest number of SNVs (3), had 5 SV, while 10 strains did not have any SV> 100bp, including 4 strains with > 10 SNVs. In addition, 5 insertion sequence (IS) insertions were identified in 3 distinct strains, one of which disrupted the *agr* locus (Table 2).

Interestingly, between the same strain CI pairs obtained from host subject 420, there was a 4638 bp deletion between T0 and T1. This deletion encompassed the cell-wall spanning region, the transmembrane region, and the cytoplasmic domain of the MSCRAMM serine-repeat *sdrC* gene, along with the signal sequence, ligand binding domain and repeat regions in the neighbouring serine-repeat *sdrD* gene as depicted in the coverage and pile-up plot shown in Figure 2B. This was leading to the recombination of the cell-wall spanning region, the transmembrane region and the cytoplasmic domain from the *sdrD* gene with the signal sequence, ligand binding domain, and repeat regions

of the sdrC gene (Fig. 2A). Additionally, in this CI pair, the fibrinogen-binding adhesin *SdrG* had a tandem duplication, and there was a tandem duplication in the extracellular adherence protein *Eap/Map* over time.

Another noteworthy observation was the identification of a large SV event between the same strain pair from host 4875. A transposon carrying the blaZ locus was lost in the second timepoints isolate (Fig. 2C). Specifically, the second timepoint isolate showed a loss of a transposon carrying the *blaZ* locus in the chromosome while simultaneously acquiring a plasmid containing the same locus (Fig. 2C and E). The coverage and pile-up plot shown in Figure 2D revealed that the coverage of the *blaZ* locus contained by the plasmid was higher compared to that of the chromosome, likely due to the high plasmid copy number (Fig. 2F). These findings highlight the dynamic nature of virulence and AMR genes that occur in persistent *S. aureus* isolates.

Plasmid carriage is common, and plasmids often encode beta-lactamase resistance genes

Hybrid long and short-read sequencing allowed us to analyse the plasmid content of these isolates and probe their change over time. Fifty-three plasmid contigs were assembled from 41/68 isolates, while the remaining 27 isolates did not carry any plasmids. 43/53 plasmid contigs were determined to be complete and circularised, while the other 10 were putative incomplete contigs. The analysis of the plasmids detected in the 68 CIs revealed a bimodal distribution of mash distances between each plasmid contig (1st quantile: 0.0, Median: 0.85, 3rd quantile: 0.94), indicating that approximately 50 plasmids had a high level of similarity (Fig. 3). Twenty plasmid contigs were identified in the 28 'same strain' isolate pairs, of which 16 (8 at each timepoint) were present in both timepoints. Plasmid gain was observed between 2 isolate pairs (subjects 3997 and 4875), where the second timepoint isolates C353 and C294 gained 1

and 2 plasmids, respectively. In contrast, plasmid loss was observed in one same strain isolate pair (5047), where the second timepoint isolate C351 lost one plasmid over time. 27/53 plasmid contigs from 26 distinct isolates carried the beta-lactamase gene *blaZ*. Of these 27 plasmids, 17/27 were deemed closely related enough to be analysed as the same plasmid based on the empirical thresholds outlined in the methods (Fig. S3). Two additional antimicrobial resistance genes were identified in plasmids: erythromycin resistance gene *ErmC* (encoded on a 2473bp plasmids common to 3 strains) and the quaternary ammonium compound resistance gene *qacA*, found on 1 20560bp plasmid.

The number of beta-lactamase encoding plasmids increased from 11 at T0 to 16 at T1, with two same strain isolates acquiring beta-lactamase resistance plasmids. In contrast, three different strain isolates present at T1 replaced isolates at T0 that did not carry a beta-lactamase plasmid, indicating a selection pressure to gain beta-lactamase resistance.

Plasmid copy numbers increase with time in the same strain group

We found a moderate positive correlation (Spearman's correlation coefficient R=0.63) between plasmid copy numbers estimated using long and short-read methods (Fig. S4A). The median plasmid copy number estimation was 1.63 times higher in the long-read dataset than in the short-read dataset. Beta-lactamase-carrying plasmids exhibited an even more noticeable difference in copy number estimation between techniques, with a median 2.29 times higher copy number estimate in the long-read dataset. The long-read dataset did not capture four plasmid contigs; however, these were all incomplete (Fig. S4B).

We further investigated the stability of plasmid copy numbers in the 'same strain' group, focusing on the eight conserved plasmids. We observed a significant increase in the copy number of the conserved plasmids over time ($p<0.05$) (Fig. 4), with 4 of the eight conserved isolates being *blaZ* positive. However, we observed no significant difference between the plasmid copy number and timepoint when we examined the short-read data.

Planktonic antibiotic susceptibility remains stable over time

The antibiotic susceptibility of all CIs was tested (n=68). Mupirocin appeared to be the most potent, with 85.2% and 67.65% of MIC values below the lowest concentration tested (0.06 mg/L) for the first and second timepoints CIs, respectively. In contrast, erythromycin and clarithromycin had lower susceptibility rates, with over 22% of CIs being resistant to each antibiotic (Table S4). Overall, doxycycline was highly effective at both timepoints, with 97% of CIs being susceptible. When comparing the first and second timepoints CIs, there was no significant difference in the proportion of resistance between the CI pairs classified in the different or same strain group (Fig. S5).

Biofilm antibiotic tolerance increases over time in persistent *S. aureus* strains

Next, we investigated the antibiotic tolerance of biofilms for all isolates. The viability results after antibiotic treatment were analysed using a GLMM. The model included the following variables: timepoint, antibiotic, antibiotic concentration, and same strain-relatedness classification. The summary statistics of the GLMM results for all effects are provided in table 1. The biofilm viability data showed high variability in antibiotic tolerance between CIs and antibiotics. Although all antibiotics significantly reduced the biofilm viability ($p<0.001$), their dose-response relationships varied. Except for doxycycline, all antibiotics reached a plateau in their antibiofilm effects at 5 mg/L, reducing biofilm viability by approximately 35%, and did not eradicate biofilms at the highest concentration (640 mg/L). Notably, mupirocin at the lowest concentration of 1.25 mg/L showed a reduction of over 50% in biofilm viability, despite not eradicating the biofilms at 640 mg/L (Fig. 5A).

Interestingly, we observed a significant increase ($p<0.001$) in antibiotic tolerance of biofilms over time between the first and second isolates classified as 'same strain' isolates compared to the first timepoint (Fig. 5B), suggesting that the same strain isolates gained tolerance over time. We then assessed the biofilm biomass using crystal violet staining to investigate the potential relationship between increased antibiotic tolerance and biofilm quantity. We observed a significant increase in the mean biomass of biofilms between the first and second timepoint CIs of the same strain group (paired Wilcoxon signed-rank test, $p < 0.05$) (Fig. 6), indicating that the increased biofilm tolerance could be due to increased biofilm production by the same strain isolates over time. A similar trend was seen for the biofilm viability results after 48 hours of growth without antibiotic treatment. Specifically, the biofilm fluorescence of the same strain isolates at the first timepoint was significantly lower than that of different strain isolates

498 ($p < 0.05$). However, the second timepoint of the same strain group showed a significant
499 increase in biofilm production ($p < 0.01$) over time, resulting in no significant difference
500 in biofilm fluorescence between the second timepoint isolates of the same strain and
501 different strain groups (Fig. S7).
502
503 Next, we investigated the potential correlation between the number of days of antibiotic
504 usage by CRS patients and the increased biofilm antibiotic tolerance. The most
505 commonly prescribed antibiotic was augmentin, but in terms of total exposure time,
506 doxycycline, followed by sinus/nasal saline irrigation mixed with mupirocin and
507 augmentin, had the most extensive antibiotic exposure in all subjects (Fig. S6). CIs
508 classified as the same and different strains had a mean exposure of 16.4 days (±7.97)
509 and 15.7 days (±8.39), respectively. However, we did not find a significant relationship
510 between the total number of days of antibiotic exposure and increased biomass between
511 CIs pairs (Spearman correlation coefficient = -0.11, $p = 0.58$).

Discussion

The current study aimed to investigate the persistence of *S. aureus* in the nasal cavity of chronically colonised CRS patients and the related genomic and phenotypic changes over time in a set of longitudinal collections of *S. aureus* CIs. Our hybrid long and short-read sequencing approach allowed us to assemble near-perfect complete genomes and conduct detailed longitudinal genomic analysis. While our study did not identify a specific gene or gene cluster that explains *S. aureus* persistence, persister isolates often show changes in mobile genetic elements such as plasmids, prophages and insertion sequences, indicating a role of the 'mobilome' in promoting persistence. The genomic adaptation of persister isolates was episode-specific, suggesting that each colonisation event may select different adaptations that enable the survival of *S. aureus* in each host. Additionally, the increase in biofilm tolerance to antibiotics over time observed in the same strain isolates shows that antibiotic tolerance of biofilm is a key pathoadaptation by persister isolates to the sinonasal environment of CRS patients.

Our study found that out of the 34 CI pairs, 14 (41%) were highly related strains based on a two-step approach considering their MLST/PopPUNK clustering and low core genome between isolate pair SNV. Past studies have posited that longitudinal follow-up of *S. aureus* nasal carriage in the healthy population colonisation by a single strain occurs between the 73% and 77% over time (Muthukrishnan et al., 2013). Additionally, Drilling et al. identified that 79% of recalcitrant CRS patients have a persistent *S. aureus* strain in their paranasal sinuses (Drilling et al., 2014). However, these results are based on MLST and pulsed-field gel electrophoresis typing, which may overestimate persister isolates due to less accuracy in discerning strains' genetic relatedness compared to WGS.

Thunberg et al. reported a lower proportion (20%) for single-strain long-term colonisation in CRS patients using WGS. This proportion is lower than the 41% identified in this study. A possible explanation for this might be a longer time between CI pairs collection (10 years) and a lower sample size (n=15) in that study (Thunberg et al., 2021). Furthermore, a considerable proportion of the isolates (35.2%) did not belong to any known CC based on MLST analysis, while 2 CIs pairs belonged to the same CC or VLKC while having relatively high SNV and SV counts between them, highlighting the limitations of this approach in characterising the genetic similarity of *S. aureus* populations.

The definition of closely related clonal isolates in the literature often employs a threshold-based approach using SNVs divergence. This is typically done by mapping short-read sequences to a reference sequence or calculating core genome SNPs. (Coll et al., 2020; Lagos et al., 2022). However, using long-read sequencing technologies enabled us to assemble near-perfect genome assemblies and plasmids instead, which facilitated using the first timepoint isolate as a reference for each longitudinal pair. This revealed that even in low SNV divergent isolate pairs, isolates undergo significant structural changes, such as prophage acquisition, mobile genetic element insertion or loss, and plasmid acquisition, that are difficult or impossible to capture using SNVs only. Additionally, we found no relationship between the number of SNVs and the presence or number of structural variants. Combined with other sequential genomics studies that have revealed similar structural changes in the context of bacteraemia, we suggest that SNP-based cutoffs cannot fully capture CIs' genomic adaptations and, instead, methods that take into account structural variation should complement the analysis (Giulieri et al., 2018; Giulieri et al., 2022).

MSCRAMM genes are known to be involved in epithelial adhesion and biofilm formation (Foster, 2019; Raafat, Otto, Reppschlager, Iqbal, & Holtfreter, 2019). While a single gene or gene cluster was not found to be indicative of colonisation, our comprehensive genomic analysis demonstrated that MSCRAMM genes frequently exhibited variability in persister strains over time, implying that selection pressure might act on the MSCRAMM genes in chronic colonisation. Interestingly, we found that persisters commonly had both small and structural MSCRAMM gene variants over time, suggesting that once colonisation has occurred, persister strains may attenuate their virulence profiles by adaptive evolution over time (Howden et al., 2023). Detailed analysis of the *sdr* locus deletion in 4875 revealed recombination of the folding domains from the *sdrC* gene and the wall-spanning and sort domain of the *sdrD* gene, suggesting that intra-host surface adhesin modulation can occur. To our knowledge, such recombination has not been previously reported in *S. aureus*. While it is known that serine-aspartate repeat MSCRAMM proteins are variable and contribute to biofilm formation (Ajayi et al., 2018; Barbu, Mackenzie, Foster, & Hook, 2014), more work needs to be done to characterise the relationship between divergent serine-aspartate repeat MSCRAMM proteins and their relationship to within-host adaptation.

We employed the Nanopore long-read Rapid Barcoding Kit library preparations, which have been demonstrated to retrieve small plasmids effectively (R. R. Wick, Judd, Wyres, & Holt, 2021). Our study revealed that *S. aureus* isolated from the sinonasal cavity of CRS patients frequently carried plasmids, regardless of their persistence. While our sample size was insufficient to establish a definitive association between plasmid carriage and lineage, we confirmed that these plasmids commonly contained the beta-lactamase gene

586 *blaZ*, which has been frequently found in *S. aureus* strains since the advent of penicillin
587 (Turner et al., 2019). Furthermore, our results suggest that *blaZ* encoding plasmids
588 become more prevalent over time, but given the limited sample size, cautious
589 interpretation is warranted.
590 Overall, our study revealed a trend of higher plasmid copy numbers in the long-read
591 dataset compared to the short-read data, consistent with the findings of Wick et al. (R. R.
592 Wick et al., 2021). We speculate that the discrepancy in copy numbers estimation in the
593 long-read dataset compared to the short may be attributed to the PCR-free nature of the
594 Rapid Barcoding Kit, which could potentially reduce bias compared to PCR-based short-
595 read methods. However, this hypothesis requires further investigation, particularly as
596 long-read sequencing becomes more commonly used, as there is scant literature on the
597 impact of different library preparations on plasmid copy number estimation. Although
598 limited knowledge exists regarding the fitness cost of carriage and copy number of
599 plasmids for *S. aureus*, our study observed an increase in the copy number of conserved
600 plasmids over time in the long-read dataset for the persistent isolates not in the short-
601 read dataset.
602
603 Consistent with previous studies, we observed a high prevalence of macrolide resistance
604 in our set of CIs isolated from CRS patients (Bhattacharyya & Kepnes, 2008).
605 Additionally, our findings are consistent with previous studies that have shown a
606 significant decrease in the effectiveness of antibiotics against *S. aureus* biofilms
607 compared to their planktonic counterparts (C. W. Hall & Mah, 2017). Only doxycycline
608 was found to have a strong ability to reduce biofilms to near eradication. However, this
609 was only at concentrations exceeding the therapeutic window in humans. These results
610 suggest that antibiotics alone may not be sufficient for eradicating *S. aureus* biofilms in

611 the sinuses of long-term colonized CRS patients, as biofilms are a common feature in the
612 sinuses of CRS patients (Foreman, Psaltis, Tan, & Wormald, 2010; Singhal, Psaltis,
613 Foreman, & Wormald, 2010). Our finding of a frequent persistence of a single *S. aureus*
614 strain in CRS patients is further evidence that the use of topical and systemic antibiotics
615 alone may not be sufficient to eradicate the bacteria. However, we observed a
616 substantial reduction of *S. aureus* biofilms for mupirocin in concentrations achievable
617 when applied topically in saline-based irrigations (Kim & Kwon, 2016). Therefore, saline
618 nasal irrigation mixed with mupirocin could play a role in the peri-operative phase of
619 functional endoscopic sinus surgery of CRS patients by reducing the *S. aureus* biofilm,
620 which has been correlated with delayed wound healing and poor post-surgical outcomes
621 (Percival, 2017; Psaltis et al., 2008).
622
623 Pathoadaptation of persistent colonisers in (chronic) inflammatory conditions has been
624 described for pathogens such as *S. aureus* and *Pseudomonas aeruginosa* (Howden et al.,
625 2023; Rossi et al., 2021). A surprising finding in this study was the significantly
626 increased biofilm antibiotic tolerance over time of the *S. aureus* strains that are
627 persistent. This increased tolerance was correlated with an increase in the biomass of
628 biofilms of the persister isolates. The biofilm production and viability in persister CIs
629 were lower compared to the non-persister strains at the first timepoint. This suggests
630 that CIs with attenuated biofilm production capacities are more likely to persist in the
631 niche. It can be postulated that the observed increased antibiotic tolerance in those
632 persistent strains over time assists them in their host adaptation, making them well-
633 equipped to occupy and dominate the sinonasal microenvironment of CRS patients,
634 which are frequently exposed to antibiotics. However, it is essential to note that the
635 sinonasal cavity of humans is a relatively low-nutrient environment for bacteria, and

high biofilm production might bring a fitness cost (Krismer et al., 2014). The increased biofilm production adaptation may arise during disease exacerbation with high bacterial load in the sinuses and antibiotic exposure. It may present a fitness cost during periods between exacerbations, allowing strains with less biofilm production to take over the niche. The data on non-persistent strains did not show a reduction in biofilm production between the first and second strains. However, the exact timepoint of strain change was not known.

Various mechanisms have been postulated to contribute to biofilm-based antibiotic tolerance of bacteria and the production of extracellular polymeric substances (C. W. Hall & Mah, 2017; Karygianni, Ren, Koo, & Thurnheer, 2020). Although we observed episode-specific mutations in the persistent isolates, we noted that genes involved in adhesion and biofilm formation were frequently affected, suggesting that the accumulation of mutations in different genes can lead to similar phenotypic adaptations.

Limitations

The findings of this study have to be seen in the light of some limitations. Since the study was limited to *S. aureus* CIs isolated from patients suffering from CRS, it was not possible to compare the results to longitudinal CIs from carriers. Longitudinal CIs from carriers with extended follow-up are practically hard to obtain. Notwithstanding this limitation, this study offers some insight into the genomic and phenotypical adaption of *S. aureus* in the sinuses of CRS patients. Furthermore, the scope of the genomic analysis in this study was limited due to the low sample size. The genomic complexity of *S. aureus* does not lend itself to genome-wide association studies in low sample size populations. A natural progression of this work is to analyse the genome of specific CIs pairs and all the in-

659 between CIs to identify a genomic target that might be involved in the phenotypical
660 adaptation.

661 **Conclusion**

662 Our findings provide insights into *S. aureus* persistence in difficult-to-treat CRS and
663 highlight the resilience of bacterial biofilms. Our results shed light on the genomic and
664 phenotypic changes associated with the persistence of *S. aureus* in chronically colonised
665 CRS patients. Further studies are needed to understand the mechanisms underlying
666 these adaptations and their potential survival benefit to identify potential targets for
667 developing new eradication strategies.

668 **References**

669 Ajayi, C., Åberg, E., Askarian, F., Sollid, J. U. E., Johannessen, M., & Hanssen, A.-M.
670 (2018). Genetic variability in the sdrD gene in Staphylococcus aureus from healthy
671 nasal carriers. *BMC Microbiology, 18*(1), 34. doi:10.1186/s12866-018-1179-7
672 Ankenbrand, T. H. a. M. J. (2022). gggenomes: A Grammar of Graphics for Comparative
673 Genomics. Retrieved from https://github.com/thackl/gggenomes
674 Barbu, E. M., Mackenzie, C., Foster, T. J., & Hook, M. (2014). SdrC induces staphylococcal
675 biofilm formation through a homophilic interaction. *Mol Microbiol, 94*(1), 172-185.
676 doi:10.1111/mmi.12750
677 Barshak, M. B., & Durand, M. L. (2017). The role of infection and antibiotics in chronic
678 rhinosinusitis. *Laryngoscope Investig Otolaryngol, 2*(1), 36-42. doi:10.1002/lio2.61
679 Bhattacharyya, N., & Kepnes, L. J. (2008). Assessment of trends in antimicrobial resistance in
680 chronic rhinosinusitis. *Ann Otol Rhinol Laryngol, 117*(6), 448-452.
681 doi:10.1177/000348940811700608
682 Bouras, G. (dnaapler). dnaapler. Retrieved from https://github.com/gbouras13/dnaapler
683 Bouras, G. (hybracter). hybracter Retrieved from https://github.com/gbouras13/hybracter
684 Bouras, G. (Plassembler). Plassembler. Retrieved from
685 https://github.com/gbouras13/plassembler
686 Brynildsrud, O., Bohlin, J., Scheffer, L., & Eldholm, V. (2016). Rapid scoring of genes in
687 microbial pan-genome-wide association studies with Scoary. *Genome Biol, 17*(1), 238.
688 doi:10.1186/s13059-016-1108-8
689 Chen, S., Zhou, Y., Chen, Y., & Gu, J. (2018). fastp: an ultra-fast all-in-one FASTQ
690 preprocessor. *Bioinformatics, 34*(17), i884-i890. doi:10.1093/bioinformatics/bty560
691 Coll, F., Raven, K. E., Knight, G. M., Blane, B., Harrison, E. M., Leek, D., . . . Peacock, S. J.
692 (2020). Definition of a genetic relatedness cutoff to exclude recent transmission of

693 meticillin-resistant Staphylococcus aureus: a genomic epidemiology analysis. *Lancet*
694 *Microbe, 1*(8), e328-e335. doi:10.1016/S2666-5247(20)30149-X
695 Danecek, P., Bonfield, J. K., Liddle, J., Marshall, J., Ohan, V., Pollard, M. O., . . . Li, H.
696 (2021). Twelve years of SAMtools and BCFtools. *GigaScience, 10*(2).
697 doi:10.1093/gigascience/giab008
698 De Coster, W., D'Hert, S., Schultz, D. T., Cruts, M., & Van Broeckhoven, C. (2018).
699 NanoPack: visualizing and processing long-read sequencing data. *Bioinformatics,*
700 *34*(15), 2666-2669. doi:10.1093/bioinformatics/bty149
701 Drilling, A., Coombs, G. W., Tan, H.-L., Pearson, J. C., Boase, S., Psaltis, A., . . . Wormald,
702 P.-J. (2014). Cousins, siblings, or copies: the genomics of recurrentStaphylococcus
703 aureusinfections in chronic rhinosinusitis. *International Forum of Allergy &*
704 *Rhinology, 4*(12), 953-960. doi:10.1002/alr.21423
705 Fokkens, W. J., Lund, V. J., Hopkins, C., Hellings, P. W., Kern, R., Reitsma, S., . . .
706 Zwetsloot, C. P. (2020). European Position Paper on Rhinosinusitis and Nasal Polyps
707 2020. *Rhinology, 58*(Suppl S29), 1-464. doi:10.4193/Rhin20.600
708 Foreman, A., Psaltis, A. J., Tan, L. W., & Wormald, P. J. (2010). Characterization of bacterial
709 and fungal biofilms in chronic rhinosinusitis. *Allergy Rhinol (Providence), 1*(1), 10.
710 doi:10.2500/ajra.2009.23.3413
711 Giulieri, S. G., Baines, S. L., Guerillot, R., Seemann, T., Goncalves da Silva, A., Schultz, M.,
712 . . . Howden, B. P. (2018). Genomic exploration of sequential clinical isolates reveals
713 a distinctive molecular signature of persistent Staphylococcus aureus bacteraemia.
714 *Genome Med, 10*(1), 65. doi:10.1186/s13073-018-0574-x
715 Giulieri, S. G., Guerillot, R., Duchene, S., Hachani, A., Daniel, D., Seemann, T., . . . Howden,
716 B. P. (2022). Niche-specific genome degradation and convergent evolution shaping

717 Staphylococcus aureus adaptation during severe infections. *eLife, 11*, e77195.
718 doi:10.7554/eLife.77195
719 Hahne, F., & Ivanek, R. (2016). Visualizing Genomic Data Using Gviz and Bioconductor. In
720 E. Mathé & S. Davis (Eds.), *Statistical Genomics: Methods and Protocols* (pp. 335-
721 351). New York, NY: Springer New York.
722 Hall, C. W., & Mah, T. F. (2017). Molecular mechanisms of biofilm-based antibiotic
723 resistance and tolerance in pathogenic bacteria. *FEMS Microbiol Rev, 41*(3), 276-301.
724 doi:10.1093/femsre/fux010
725 Hall, M. (2022). Rasusa: Randomly subsample sequencing reads to a specified coverage.
726 *Journal of open source software, 7*(69), 3941. doi:10.21105/joss.03941
727 Hastan, D., Fokkens, W. J., Bachert, C., Newson, R. B., Bislimovska, J., Bockelbrink, A., . . .
728 Burney, P. (2011). Chronic rhinosinusitis in Europe--an underestimated disease. A
729 GA(2)LEN study. *Allergy, 66*(9), 1216-1223. doi:10.1111/j.1398-9995.2011.02646.x
730 Hawkey, J., Wyres, K. L., Judd, L. M., Harshegyi, T., Blakeway, L., Wick, R. R., . . . Holt, K.
731 E. (2022). ESBL plasmids in Klebsiella pneumoniae: diversity, transmission and
732 contribution to infection burden in the hospital setting. *Genome Med, 14*(1), 97.
733 doi:10.1186/s13073-022-01103-0
734 Hoggard, M., Wagner Mackenzie, B., Jain, R., Taylor, M. W., Biswas, K., & Douglas, R. G.
735 (2017). Chronic Rhinosinusitis and the Evolving Understanding of Microbial Ecology
736 in Chronic Inflammatory Mucosal Disease. *Clinical Microbiology Reviews, 30*(1),
737 321. doi:10.1128/CMR.00060-16
738 Hopkins, C. (2019). Chronic Rhinosinusitis with Nasal Polyps. *N Engl J Med, 381*(1), 55-63.
739 doi:10.1056/NEJMcp1800215

740 Howden, B. P., Giulieri, S. G., Wong Fok Lung, T., Baines, S. L., Sharkey, L. K., Lee, J. Y.
741 H., . . . Stinear, T. P. (2023). Staphylococcus aureus host interactions and adaptation.
742 *Nature Reviews Microbiology*. doi:10.1038/s41579-023-00852-y
743 Jia, B., Raphenya, A. R., Alcock, B., Waglechner, N., Guo, P., Tsang, K. K., . . . McArthur,
744 A. G. (2017). CARD 2017: expansion and model-centric curation of the
745 comprehensive antibiotic resistance database. *Nucleic Acids Res, 45*(D1), D566-D573.
746 doi:10.1093/nar/gkw1004
747 Jolley, K. A., Bray, J. E., & Maiden, M. C. J. (2018). Open-access bacterial population
748 genomics: BIGSdb software, the PubMLST.org website and their applications.
749 *Wellcome Open Res, 3*, 124. doi:10.12688/wellcomeopenres.14826.1
750 Karygianni, L., Ren, Z., Koo, H., & Thurnheer, T. (2020). Biofilm Matrixome: Extracellular
751 Components in Structured Microbial Communities. *Trends Microbiol, 28*(8), 668-681.
752 doi:10.1016/j.tim.2020.03.016
753 Khelik, K., Lagesen, K., Sandve, G. K., Rognes, T., & Nederbragt, A. J. (2017). NucDiff: in-
754 depth characterization and annotation of differences between two sets of DNA
755 sequences. *BMC Bioinformatics, 18*(1), 338. doi:10.1186/s12859-017-1748-z
756 Kim, J. S., & Kwon, S. H. (2016). Mupirocin in the Treatment of Staphylococcal Infections in
757 Chronic Rhinosinusitis: A Meta-Analysis. *PLOS ONE, 11*(12), e0167369.
758 doi:10.1371/journal.pone.0167369
759 Kolmogorov, M., Yuan, J., Lin, Y., & Pevzner, P. A. (2019). Assembly of long, error-prone
760 reads using repeat graphs. *Nat Biotechnol, 37*(5), 540-546. doi:10.1038/s41587-019-
761 0072-8
762 Krismer, B., Liebeke, M., Janek, D., Nega, M., Rautenberg, M., Hornig, G., . . . Peschel, A.
763 (2014). Nutrient limitation governs Staphylococcus aureus metabolism and niche

764 adaptation in the human nose. *PLoS Pathog, 10*(1), e1003862.
765 doi:10.1371/journal.ppat.1003862
766 Krysko, O., Teufelberger, A., Van Nevel, S., Krysko, D. V., & Bachert, C. (2019).
767 Protease/antiprotease network in allergy: The role of Staphylococcus aureus protease-
768 like proteins. *Allergy, 74*(11), 2077-2086. doi:10.1111/all.13783
769 Lagos, A. C., Sundqvist, M., Dyrkell, F., Stegger, M., Soderquist, B., & Molling, P. (2022).
770 Evaluation of within-host evolution of methicillin-resistant Staphylococcus aureus
771 (MRSA) by comparing cgMLST and SNP analysis approaches. *Sci Rep, 12*(1), 10541.
772 doi:10.1038/s41598-022-14640-w
773 Lees, J. A., Harris, S. R., Tonkin-Hill, G., Gladstone, R. A., Lo, S. W., Weiser, J. N., . . .
774 Croucher, N. J. (2019). Fast and flexible bacterial genomic epidemiology with
775 PopPUNK. *Genome Res, 29*(2), 304-316. doi:10.1101/gr.241455.118
776 Li, H. (2013). Aligning sequence reads, clone sequences and assembly contigs with BWA-
777 MEM. *arXiv preprint arXiv:1303.3997*.
778 Li, H. (2018). Minimap2: pairwise alignment for nucleotide sequences. *Bioinformatics,*
779 *34*(18), 3094-3100. doi:10.1093/bioinformatics/bty191
780 Liu, B., Zheng, D., Jin, Q., Chen, L., & Yang, J. (2019). VFDB 2019: a comparative
781 pathogenomic platform with an interactive web interface. *Nucleic Acids Res, 47*(D1),
782 D687-D692. doi:10.1093/nar/gky1080
783 Mah, T. F. (2014). Establishing the minimal bactericidal concentration of an antimicrobial
784 agent for planktonic cells (MBC-P) and biofilm cells (MBC-B). *J Vis Exp*(83),
785 e50854. doi:10.3791/50854
786 Molder, F., Jablonski, K. P., Letcher, B., Hall, M. B., Tomkins-Tinch, C. H., Sochat, V., . . .
787 Koster, J. (2021). Sustainable data analysis with Snakemake. *F1000Res, 10*, 33.
788 doi:10.12688/f1000research.29032.2

789 Muthukrishnan, G., Lamers, R. P., Ellis, A., Paramanandam, V., Persaud, A. B., Tafur, S., . . .
790 Cole, A. M. (2013). Longitudinal genetic analyses of Staphylococcus aureus nasal
791 carriage dynamics in a diverse population. *BMC Infect Dis, 13*(1), 221.
792 doi:10.1186/1471-2334-13-221
793 Nepal, R., Houtak, G., Shaghayegh, G., Bouras, G., Shearwin, K., Psaltis, A. J., . . . Vreugde,
794 S. (2021). Prophages encoding human immune evasion cluster genes are enriched in
795 Staphylococcus aureus isolated from chronic rhinosinusitis patients with nasal polyps.
796 *Microb Genom, 7*(12). doi:10.1099/mgen.0.000726
797 Okifo, O., Ray, A., & Gudis, D. A. (2022). The Microbiology of Acute Exacerbations in
798 Chronic Rhinosinusitis - A Systematic Review. *Front Cell Infect Microbiol, 12*,
799 858196. doi:10.3389/fcimb.2022.858196
800 Ondov, B. D., Treangen, T. J., Melsted, P., Mallonee, A. B., Bergman, N. H., Koren, S., &
801 Phillippy, A. M. (2016). Mash: fast genome and metagenome distance estimation
802 using MinHash. *Genome Biol, 17*(1), 132. doi:10.1186/s13059-016-0997-x
803 ONT. (2022). Medaka. Retrieved from https://github.com/nanoporetech/medaka
804 Percival, S. L. (2017). Importance of biofilm formation in surgical infection. *Br J Surg,*
805 *104*(2), e85-e94. doi:10.1002/bjs.10433
806 Petit, R. A., 3rd, & Read, T. D. (2018). Staphylococcus aureus viewed from the perspective of
807 40,000+ genomes. *PeerJ, 6*, e5261. doi:10.7717/peerj.5261
808 Pettit, R. K., Weber, C. A., Kean, M. J., Hoffmann, H., Pettit, G. R., Tan, R., . . . Horton, M.
809 L. (2005). Microplate Alamar blue assay for Staphylococcus epidermidis biofilm
810 susceptibility testing. *Antimicrob Agents Chemother, 49*(7), 2612-2617.
811 doi:10.1128/AAC.49.7.2612-2617.2005

812 Psaltis, A. J., Weitzel, E. K., Ha, K. R., & Wormald, P. J. (2008). The effect of bacterial
813 biofilms on post-sinus surgical outcomes. *American journal of rhinology, 22*(1), 1-6.
814 doi:10.2500/ajr.2008.22.3119
815 R Core Team. (2017). R: A language and environment for statistical computing. R Foundation
816 for Statistical Computing, Vienna, Austria.
817 Roach, M. J., Pierce-Ward, N. T., Suchecki, R., Mallawaarachchi, V., Papudeshi, B.,
818 Handley, S. A., . . . Edwards, R. A. (2022). Ten simple rules and a template for
819 creating workflows-as-applications. *PLOS Computational Biology, 18*(12), e1010705.
820 doi:10.1371/journal.pcbi.1010705
821 Robertson, J., & Nash, J. H. E. (2018). MOB-suite: software tools for clustering,
822 reconstruction and typing of plasmids from draft assemblies. *Microb Genom, 4*(8).
823 doi:10.1099/mgen.0.000206
824 Rossi, E., La Rosa, R., Bartell, J. A., Marvig, R. L., Haagensen, J. A. J., Sommer, L. M., . . .
825 Johansen, H. K. (2021). Pseudomonas aeruginosa adaptation and evolution in patients
826 with cystic fibrosis. *Nat Rev Microbiol, 19*(5), 331-342. doi:10.1038/s41579-020-
827 00477-5
828 Schechner, V., Temkin, E., Harbarth, S., Carmeli, Y., & Schwaber, M. J. (2013).
829 Epidemiological interpretation of studies examining the effect of antibiotic usage on
830 resistance. *Clin Microbiol Rev, 26*(2), 289-307. doi:10.1128/CMR.00001-13
831 Schwengers, O., Jelonek, L., Dieckmann, M. A., Beyvers, S., Blom, J., & Goesmann, A.
832 (2021). Bakta: rapid and standardized annotation of bacterial genomes via alignment-
833 free sequence identification. *Microb Genom, 7*(11). doi:10.1099/mgen.0.000685
834 Sedlazeck, F. J., Rescheneder, P., Smolka, M., Fang, H., Nattestad, M., von Haeseler, A., &
835 Schatz, M. C. (2018). Accurate detection of complex structural variations using

single-molecule sequencing. *Nat Methods, 15*(6), 461-468. doi:10.1038/s41592-018-0001-7

Seemann, T. (2015). Snippy: fast bacterial variant calling from NGS reads Retrieved from https://github.com/tseemann/snippy

Seemann, T. (Abricate). Abricate. Retrieved from https://github.com/tseemann/abricate

Seemann, T. (mlst). mlst. Retrieved from https://github.com/tseemann/mlst

Shaghayegh, G., Cooksley, C., Bouras, G. S., Panchatcharam, B. S., Idrizi, R., Jana, M., . . . Vreugde, S. (2023). Chronic rhinosinusitis patients display an aberrant immune cell localization with enhanced S aureus biofilm metabolic activity and biomass. *Journal of Allergy and Clinical Immunology, 151*(3), 723-736.e716. doi:10.1016/j.jaci.2022.08.031

Singhal, D., Foreman, A., Jervis-Bardy, J., & Wormald, P. J. (2011). Staphylococcus aureus biofilms: Nemesis of endoscopic sinus surgery. *Laryngoscope, 121*(7), 1578-1583. doi:10.1002/lary.21805

Singhal, D., Psaltis, A. J., Foreman, A., & Wormald, P. J. (2010). The impact of biofilms on outcomes after endoscopic sinus surgery. *Am J Rhinol Allergy, 24*(3), 169-174. doi:10.2500/ajra.2010.24.3462

Stiefel, P., Rosenberg, U., Schneider, J., Mauerhofer, S., Maniura-Weber, K., & Ren, Q. (2016). Is biofilm removal properly assessed? Comparison of different quantification methods in a 96-well plate system. *Appl Microbiol Biotechnol, 100*(9), 4135-4145. doi:10.1007/s00253-016-7396-9

Thunberg, U., Hugosson, S., Ehricht, R., Monecke, S., Müller, E., Cao, Y., . . . Söderquist, B. (2021). Long-Term Sinonasal Carriage of Staphylococcus aureus and Anti-Staphylococcal Humoral Immune Response in Patients with Chronic Rhinosinusitis. *Microorganisms, 9*(2), 256. doi:10.3390/microorganisms9020256

Tonkin-Hill, G., MacAlasdair, N., Ruis, C., Weimann, A., Horesh, G., Lees, J. A., . . . Parkhill, J. (2020). Producing polished prokaryotic pangenomes with the Panaroo pipeline. *Genome Biol, 21*(1), 180. doi:10.1186/s13059-020-02090-4

Turner, N. A., Sharma-Kuinkel, B. K., Maskarinec, S. A., Eichenberger, E. M., Shah, P. P., Carugati, M., . . . Fowler, V. G., Jr. (2019). Methicillin-resistant Staphylococcus aureus: an overview of basic and clinical research. *Nat Rev Microbiol, 17*(4), 203-218. doi:10.1038/s41579-018-0147-4

Vickery, T. W., Ramakrishnan, V. R., & Suh, J. D. (2019). The Role of Staphylococcus aureus in Patients with Chronic Sinusitis and Nasal Polyposis. *Curr Allergy Asthma Rep, 19*(4), 21. doi:10.1007/s11882-019-0853-7

Wick, R. R. (Porechop). Porechop. Retrieved from https://github.com/rrwick/Porechop

Wick, R. R., & Holt, K. E. (2022). Polypolish: Short-read polishing of long-read bacterial genome assemblies. *PLoS Comput Biol, 18*(1), e1009802. doi:10.1371/journal.pcbi.1009802

Wick, R. R., Judd, L. M., Gorrie, C. L., & Holt, K. E. (2017). Unicycler: Resolving bacterial genome assemblies from short and long sequencing reads. *PLoS Comput Biol, 13*(6), e1005595. doi:10.1371/journal.pcbi.1005595

Wick, R. R., Judd, L. M., Wyres, K. L., & Holt, K. E. (2021). Recovery of small plasmid sequences via Oxford Nanopore sequencing. *Microb Genom, 7*(8). doi:10.1099/mgen.0.000631

Xu, S., Li, L., Luo, X., Chen, M., Tang, W., Zhan, L., . . . Yu, G. (2022). Ggtree : A serialized data object for visualization of a phylogenetic tree and annotation data. *iMeta, 1*(4), e56. doi:10.1002/imt2.56

884 Zimin, A. V., & Salzberg, S. L. (2020). The genome polishing tool POLCA makes fast and
885 accurate corrections in genome assemblies. *PLoS Comput Biol, 16*(6), e1007981.
886 doi:10.1371/journal.pcbi.1007981
887

Tables

889 **Table 1. General linear mixed-effect model of biofilm viability**

	fluorescence				
Predictors	*Estimates*	*std. Error*	*std. Beta*	*standardised std. Error*	*p*
(Intercept)	9521.99	468.05	1.47	0.16	***
group [T1]	80.34	69.10	0.03	0.02	NS
same strain [Yes]	-732.07	642.38	-0.26	0.23	NS
concentration [1.25]	-2151.71	247.48	-0.76	0.09	***
concentration [2.5]	-2993.73	247.48	-1.05	0.09	***
concentration [5]	-3375.66	247.48	-1.19	0.09	***
concentration [10]	-3468.68	247.48	-1.22	0.09	***
concentration [20]	-3504.01	247.48	-1.23	0.09	***
concentration [40]	-3664.02	247.48	-1.29	0.09	***
concentration [80]	-3865.20	247.48	-1.36	0.09	***
concentration [160]	-3876.89	247.48	-1.37	0.09	***
concentration [320]	-4123.81	247.48	-1.45	0.09	***
concentration [640]	-3970.43	247.48	-1.40	0.09	***
antibiotic[clarithromycin]	-913.07	99.85	-0.32	0.04	***
antibiotic [clindamycin]	-940.96	99.85	-0.33	0.04	***
antibiotic [doxycycline]	-2226.13	99.85	-0.78	0.04	***
antibiotic [erythromycin]	465.69	99.85	0.16	0.04	***
antibiotic [gentamicin]	-234.94	99.85	-0.08	0.04	*
antibiotic [mupirocin]	-1526.72	99.85	-0.54	0.04	***
group [T1] Ã— same strain [Yes]	1475.91	107.68	0.52	0.04	***
Random Effects					
σ^2	3389981.04				
$\tau_{00\ id}$	3350609.42				
N_{id}	34				
Observations	4828				
Marginal R^2 / Conditional R^2	0.184 / 0.590				
					**** p<0.05 ** p<0.01 *** p<0.001***

890

891 **Table 2. SNV and SV count between same strain isolate pairs**

892

Host ID CI pair	SNV count (Snippy)	SV count (Nucdiff)	SV count (Sniffles)
1415	2	1	2
1676	3	1	1
1992	6	4	3
3344	13	0	1
3997	22	0	2
420	69	5	5
4681	6	2	1
4875	20	7	5
5047	18	1	2
5060	5	0	0
5142	3	0	0
5519	10	2	1
5562	3	11	8
5728	42	3	4

893 SNV, Single nucleotide variant; SV, Structural Variant

894 **Table S1. Biosample accession number for each sample**

895

Biosample accession	Sample id	Host id and timepoint
SAMN32360832	C22	420_T0
SAMN32360833	C265	1415_T0
SAMN32360834	C13	1676_T0
SAMN32360835	C80	1992_T0
SAMN32360836	C295	2911_T1
SAMN32360837	C52	3344_T0
SAMN32360838	C9	3997_T0
SAMN32360839	C3	4681_T0
SAMN32360840	C67	4875_T0
SAMN32360841	C72	5047_T0
SAMN32360842	C45	5142_T0
SAMN32360843	C224	5519_T0
SAMN32360844	C222	5562_T0
SAMN32360845	C241	5728_T0
SAMN32360846	C100	276_T0
SAMN32360847	C364	276_T1
SAMN32360848	C320	420_T1
SAMN32360849	C235	539_T0
SAMN32360850	C318	539_T1
SAMN32360851	C148	1170_T1
SAMN32360852	C79	1170_T0
SAMN32360853	C324	1415_T1
SAMN32360854	C76	1676_T1
SAMN32360855	C208	1992_T1
SAMN32360856	C240	2911_T0
SAMN32360857	C113	3344_T1
SAMN32360858	C195	3357_T1
SAMN32360859	C24	3357_T0
SAMN32360860	C353	3997_T1
SAMN32360861	C121	4009_T0
SAMN32360862	C255	4009_T1
SAMN32360863	C56	4681_T1
SAMN32360864	C188	4747_T1
SAMN32360865	C32	4747_T0
SAMN32360866	C16	4784_T0
SAMN32360867	C70	4784_T1
SAMN32360868	C294	4875_T1
SAMN32360869	C21	4986_T0

SAMN32360870	C273	4986_T1
SAMN32360871	C351	5047_T1
SAMN32360872	C133	5060_T0
SAMN32360873	C179	5060_T1
SAMN32360874	C149	5142_T1
SAMN32360875	C209	5308_T1
SAMN32360876	C91	5308_T0
SAMN32360877	C206	5328_T0
SAMN32360878	C276	5328_T1
SAMN32360879	C136	5390_T0
SAMN32360880	C197	5390_T1
SAMN32360881	C155	5448_T0
SAMN32360882	C339	5448_T1
SAMN32360883	C196	5469_T0
SAMN32360884	C342	5469_T1
SAMN32360885	C183	5485_T0
SAMN32360886	C312	5485_T1
SAMN32360887	C182	5503_T0
SAMN32360888	C233	5503_T1
SAMN32360889	C349	5519_T1
SAMN32360890	C333	5562_T1
SAMN32360891	C245	5631_T0
SAMN32360892	C314	5631_T1
SAMN32360893	C285	5647_T0
SAMN32360894	C355	5647_T1
SAMN32360895	C309	5728_T1
SAMN32360896	C325	5767_T0
SAMN32360897	C363	5767_T1
SAMN32360898	C311	5911_T0
SAMN32360899	C357	5911_T1

896

Table S2. Metadata characteristics of chronic rhinosinusitis subjects and corresponding clinical isolate collection

Characteristic	CRSwNP	CRSsNP	Total
Host subjects-N	29	5	34
Gender male-N	12	2	14
Age -year (± SD)	51 (± 11)	54 (± 21)	52 (± 15)
Aspirin sensitivity-N	6	0	6
Asthmatic-N	17	2	19
Mean time between CI pair collection- days (± SD)	565 (±398)	558 (±362)	563 (±387)

CRSwNP, chronic rhinosinusitis with nasal polyps, CRSsNP, chronic rhinosinusitis without nasal polyps.

Table S3. Compilation of metadata characteristics of clinical isolate by relatedness classification and host characteristics

Characteristic	Same strain pairs	Different strain pairs	Total
Count-N (% of total)	14 (41%)	20 (59%)	34 (100%)
Gender of host-Male-N	5	9	14
Age of host -year (± SD)	57 (± 15)	50 (± 16)	52 (± 15)
Phenotype of host-CRSwNP- N	14	15	29
Aspirin sensitivity of host-N	3	3	6
Asthma status of host-N	7	12	19
Mean time between CI pair collection- days (± SD)	629 (±474)	518 (±320)	563(±387)

CRSwNP, chronic rhinosinusitis with nasal polyps.

Table S4. Frequency distribution of *Staphylococcus aureus* isolates' Minimum Inhibitory Concentration (MIC)

Antibiotic	Timepoint *	MIC (%) Concentration (mg/L)												MIC_{50}	MIC_{90}	Resistant (%)
		<0.06	0.06	0.125	0.25	0.5	1	2	4	8	16	32	>32			
Erythromycin	T0	0.00	0.00	0.00	0.00	0.00	14.71	47.06	17.65	5.88	5.88	2.94	5.88	2	>32	21
	T1	0.00	0.00	0.00	0.00	0.00	2.94	38.24	26.47	14.71	2.94	5.88	8.82	4	>32	32
Doxycycline	T0	0.00	2.94	26.47	52.94	8.82	5.88	0.00	2.94	0.00	0.00	0.00	0.00	0.25	0.50	0
	T1	0.00	0.00	5.88	29.41	47.06	5.88	2.94	5.88	0.00	2.94	0.00	0.00	0.50	2	3
Clindamycin	T0	0.00	0.00	2.94	52.94	35.29	5.88	0.00	0.00	0.00	0.00	0.00	2.94	0.25	0.50	3
	T1	0.00	0.00	0.00	23.53	58.82	5.88	0.00	0.00	0.00	0.00	0.00	11.76	0.50	2	12
Augmentin	T0	0.00	0.00	0.00	5.88	14.71	38.24	32.35	2.94	0.00	5.88	0.00	0.00	4	8	N. A
	T1	0.00	0.00	0.00	2.94	8.82	23.53	29.41	11.76	5.88	5.88	8.82	2.94	4	16	N. A
Gentamycin	T0	0.00	0.00	0.00	2.94	17.65	29.41	35.29	2.94	5.88	2.94	0.00	2.94	4	16	6
	T1	0.00	0.00	0.00	0.00	2.94	11.76	41.18	14.71	11.76	5.88	2.94	8.82	4	16	18
Mupirocin	T0	85.29	2.94	8.82	0.00	0.00	0.00	0.00	0.00	0.00	2.94	0.00	0.00	<0.06	0.125	N. A
	T1	67.65	0.00	29.41	2.94	0.00	0.00	0.00	0.00	0.00	0.00	0.00	0.00	<0.06	0.125	N. A
Clarithromycin	T0	0.00	0.00	0.00	0.00	0.00	8.82	58.82	14.71	0.00	5.88	2.94	8.82	2	32	18
	T1	2.94	0.00	0.00	0.00	0.00	14.71	32.35	23.53	5.88	2.94	2.94	14.71	2	>32	26

*T0 and T1 represent the first and second CIs of the longitudinal *S. aureus* pairs. The light-grey fill represents the intermediate susceptible range, and the dark-grey fill represents the resistant range. MIC50 and MIC90 is the minimum inhibitory concentration

907 (mg/L) that inhibited 50 and 90% of the isolates, respectively. Antibiotics without shading have no interpretive MIC breakpoint
908 accessible.

Figure

Figure 1

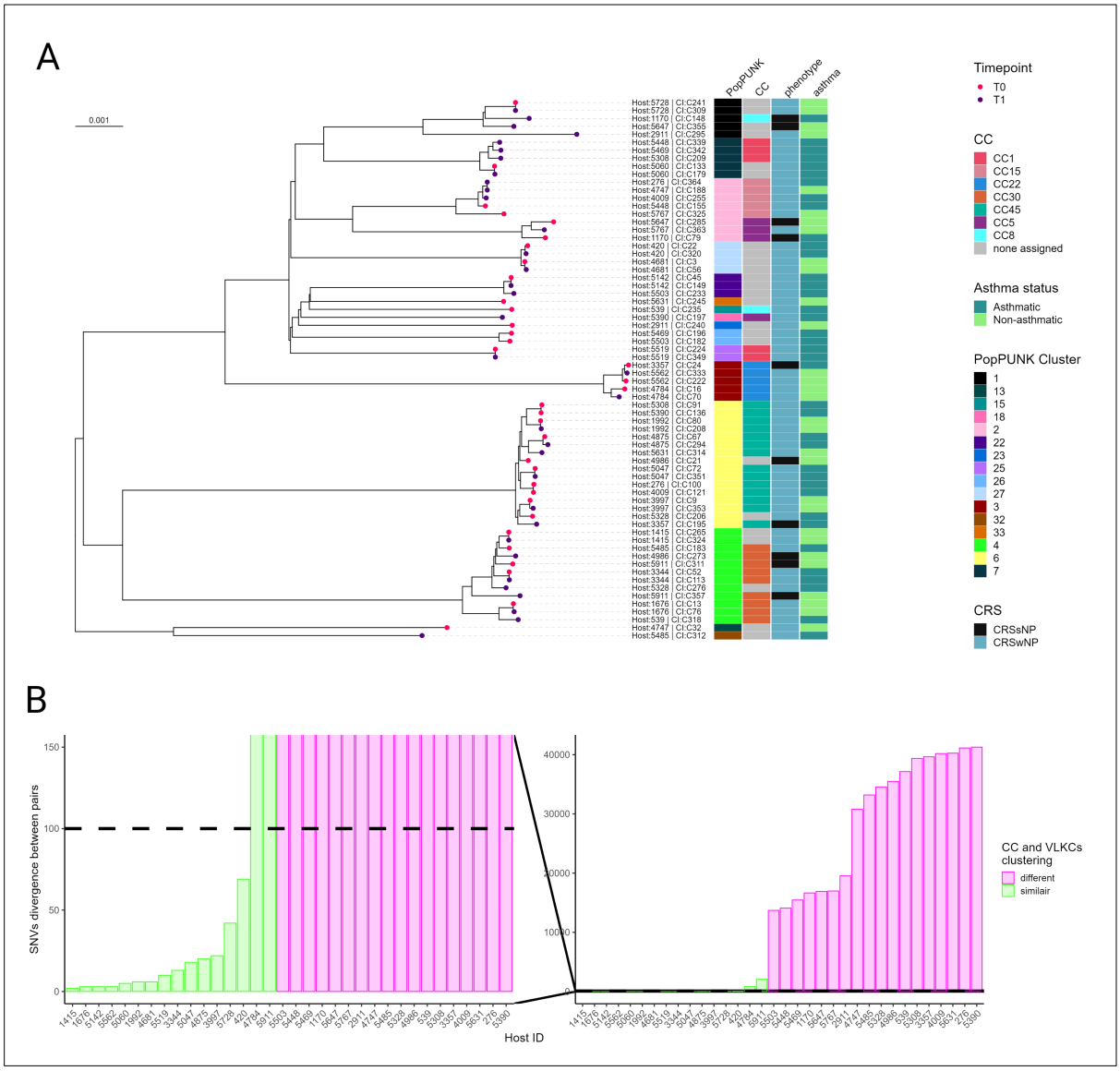

Figure 1. Genome-based classification of *Staphylococcus aureus* clinical isolates. (A) A variable-length-k-mer cluster (VLKC) midpoint rooted tree of 68 *S. aureus* genomes collected from 34 subjects with chronic rhinosinusitis (2 samples per subject) based on PopPUNK analysis. The branch tip colours represent the collection timepoint (T0= first, T1=later timepoint). The PopPUNK cluster, clonal complex (CC), CRS phenotype, and

asthma status are indicated by colour on the right side. The branch labels show the corresponding host ID and the CI number. (B) A histogram depicting the distribution of pairwise single-nucleotide variant (SNV) divergence in the core genome for all clinical isolate pairs (n=34), with colours indicating CC and VLKC similarity. The horizontal line indicates the SNV threshold used to classify pairs as either "same strain" or "different strain".

Figure 2

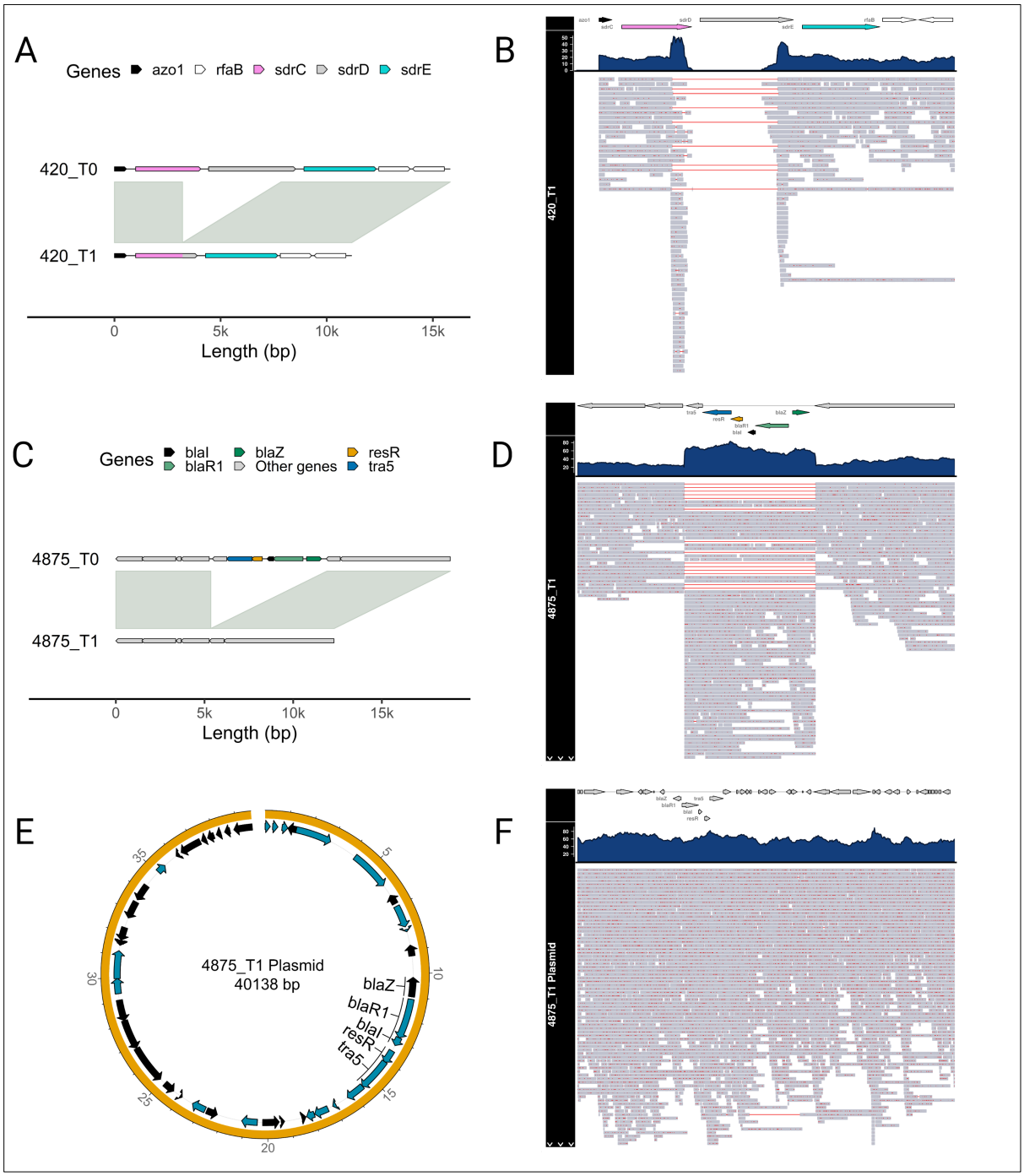

Figure 2. Structural variants identified between same strain longitudinal pairs. (A) Alignment of the *sdrCDE* locus between two isolates from the same host (420) at different timepoints. Genes are highlighted in different colours, and synteny and sequence similarity are indicated by grey fills connecting the chromosomes. The genomes of the first and second timepoint isolates are shown on top and bottom,

930 respectively. (B) Coverage and pile-up plot of aligned long-reads of the second timepoint
931 isolate of host 420 against the *sdrCDE* locus of the first timepoint isolate, red indicates
932 deleted regions in the reads. (C) Alignment of the *β-lactamase* locus between two
933 isolates from the same host (4875) at different timepoints. (D) Coverage and pile-up plot
934 of aligned long-reads of the second timepoint isolate of host 4875 against the *β-*
935 *lactamase* locus of the first timepoint isolate, red indicates deleted regions in the reads.
936 (E) Circular plot of the acquired plasmid of the second timepoint isolate of host 4875.
937 (F) Coverage and pile-up plot of aligned long-reads of the acquired plasmid of the
938 second timepoint isolate of host 4875, red indicates deleted regions in the reads.

939 **Figure 3**

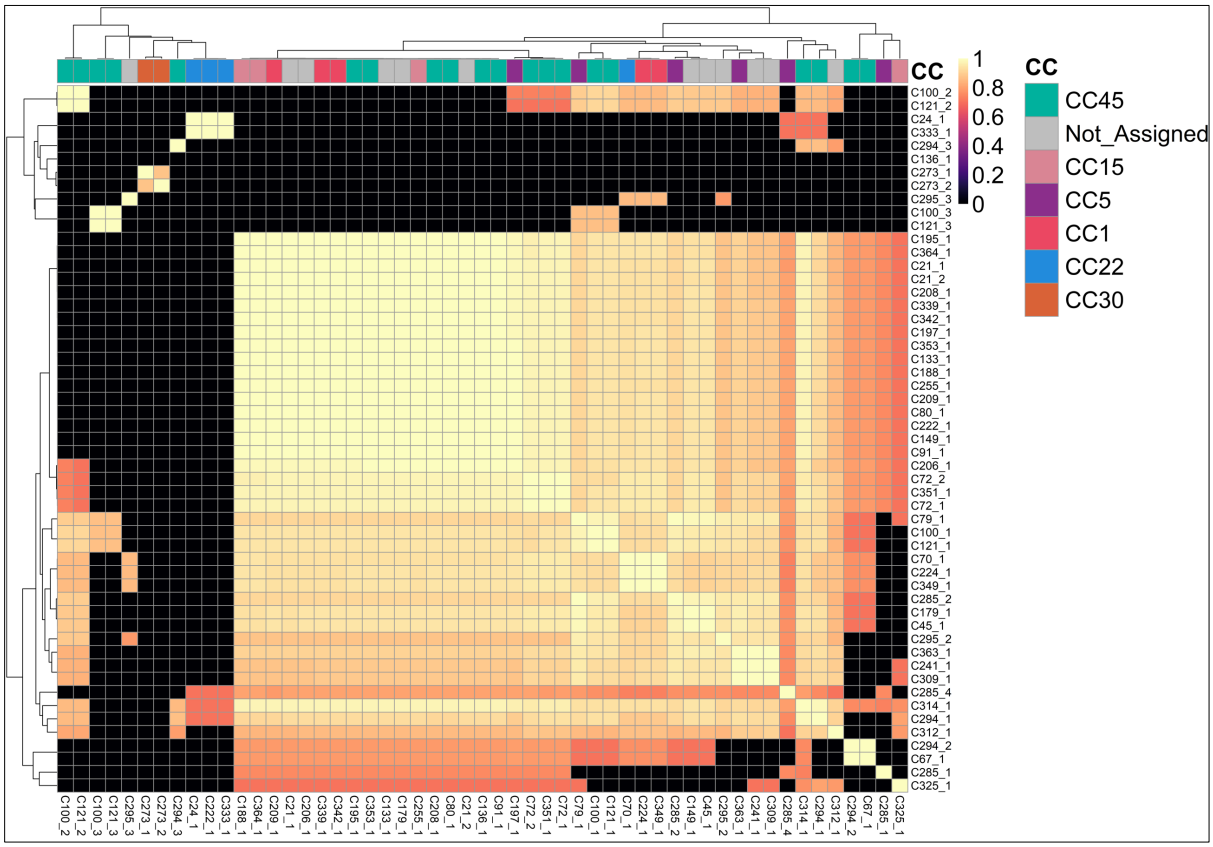

940

941 Figure 3. Heatmap displaying the minhash (Mash) distances between the 53 plasmids

942 identified in the 68 CIs. The distances were calculated using mash v2.3 and are

943 represented by a colour gradient. The clonal complex of the CI from which the plasmid

944 was recovered is indicated at the top of the heatmap.

945 **Figure 4**

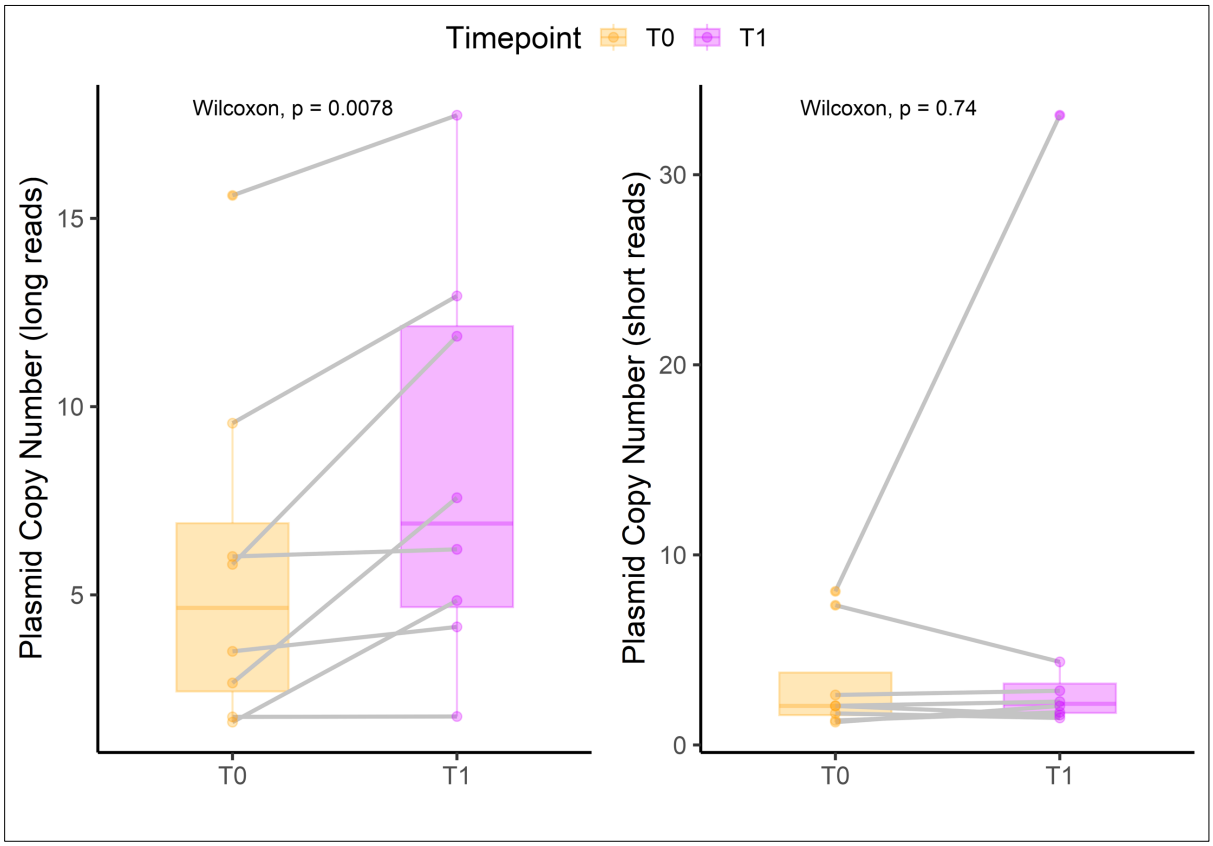

946

947 Figure 4. Copy numbers of the conserved plasmids in the 'same strain' group (n=8) for
948 short-read and long-read data. The colour indicates timepoints, and the grey line
949 indicates paired conserved plasmids. The Wilcoxon signed-rank test compared the copy
950 numbers between the two timepoints, with $p<0.05$ considered significant.

951 **Figure 5**

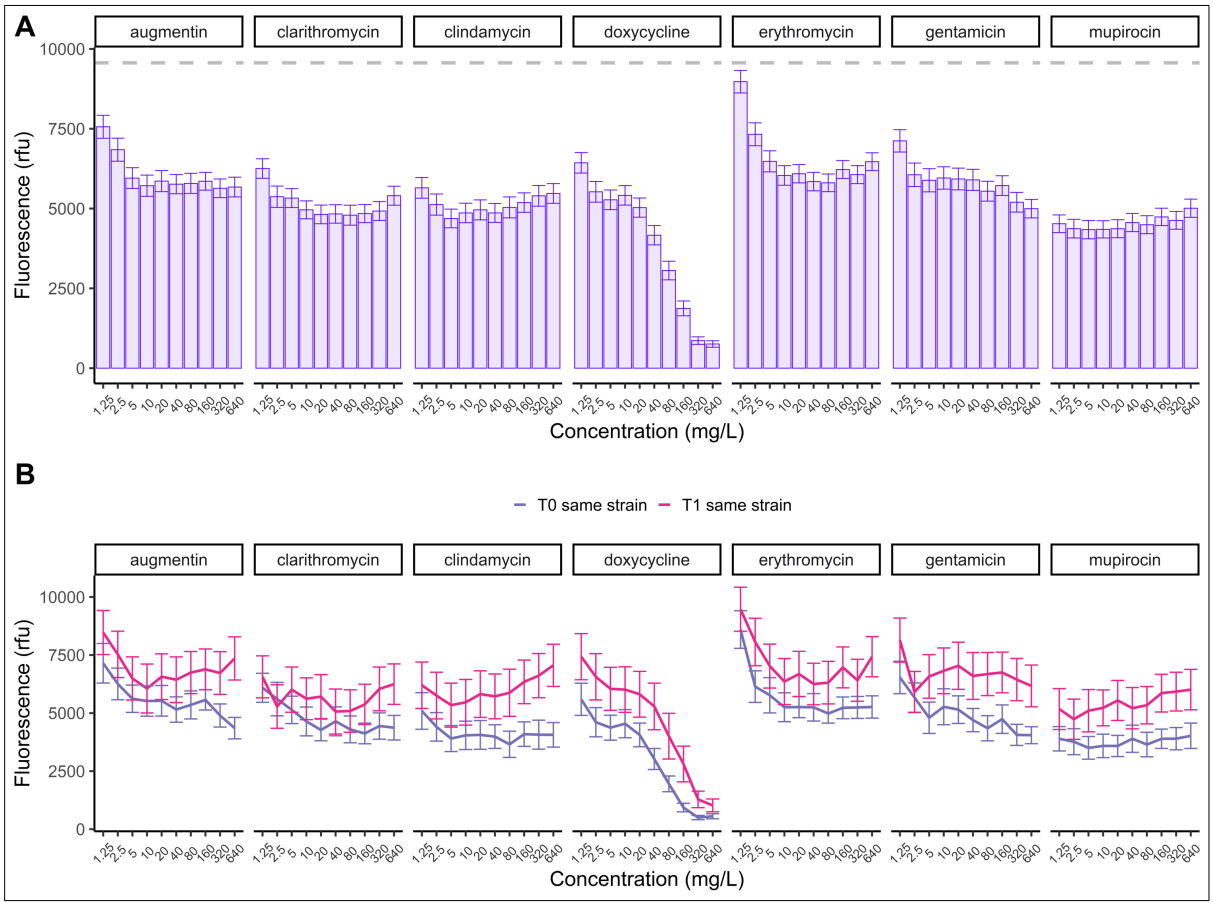

952

953 Figure 5. Tolerance of *S. aureus* biofilms to antibiotics. (A) Mean biofilm viability after
954 treatment per antibiotic and concentration in relative fluorescence units (rfu) for all 68
955 CIs. The grey dashed line represents the mean viability of isolates untreated. (B) Mean
956 biofilm viability of the first and second CIs pairs classified as the same strain after
957 treatment with increasing concentrations of antibiotics. Error bars represent the
958 standard error of the mean (SEM).

959 **Figure 6**

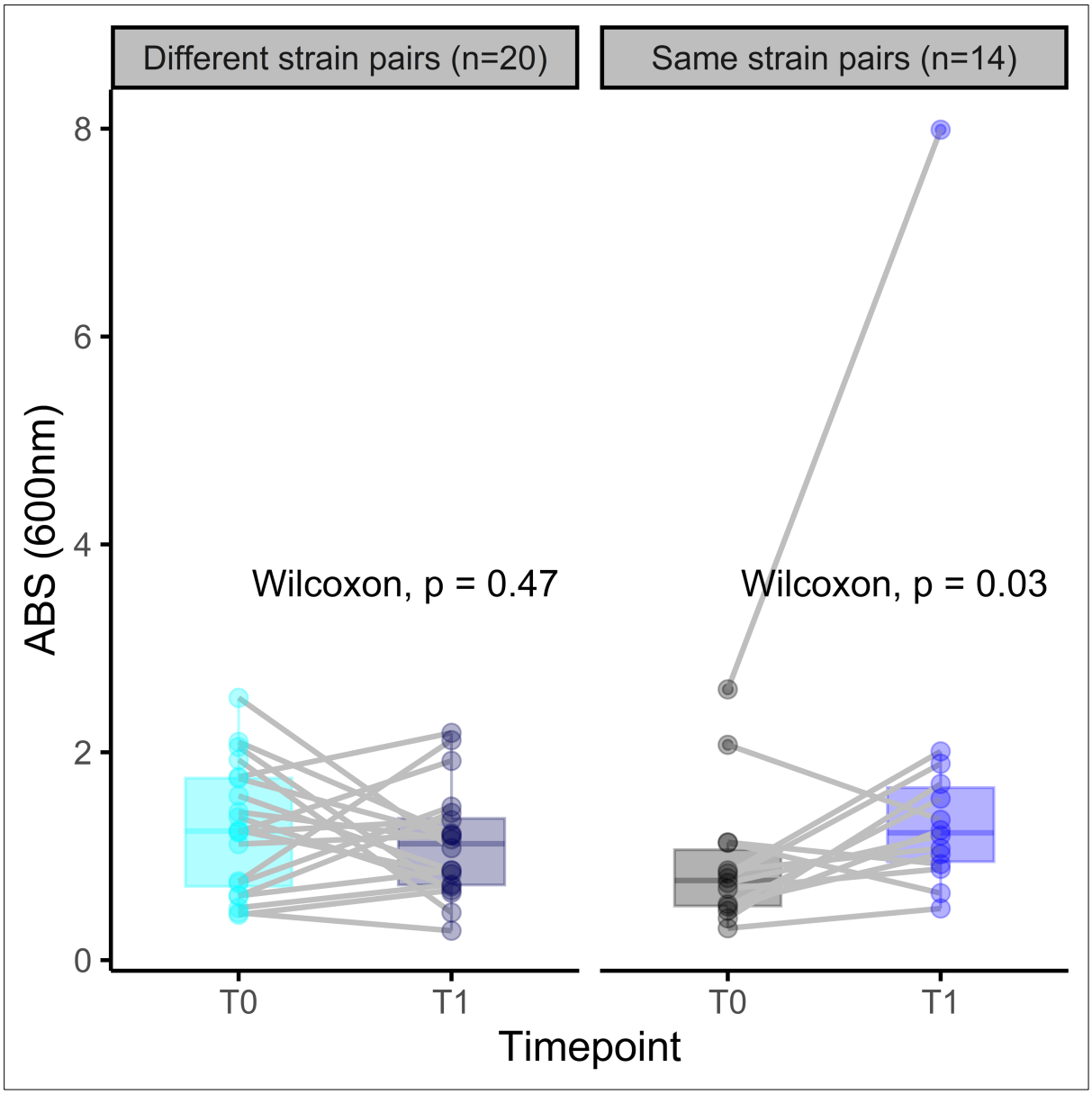

960

961 Figure 6. Biomass of *S. aureus* biofilms classified as same strain and different strain

962 using the crystal violet assay. The CIs pairs are connected with a grey line. Paired

963 Wilcoxon test was used to determine the significance between the first and second

964 timepoint.

965

966 **Figure S1**

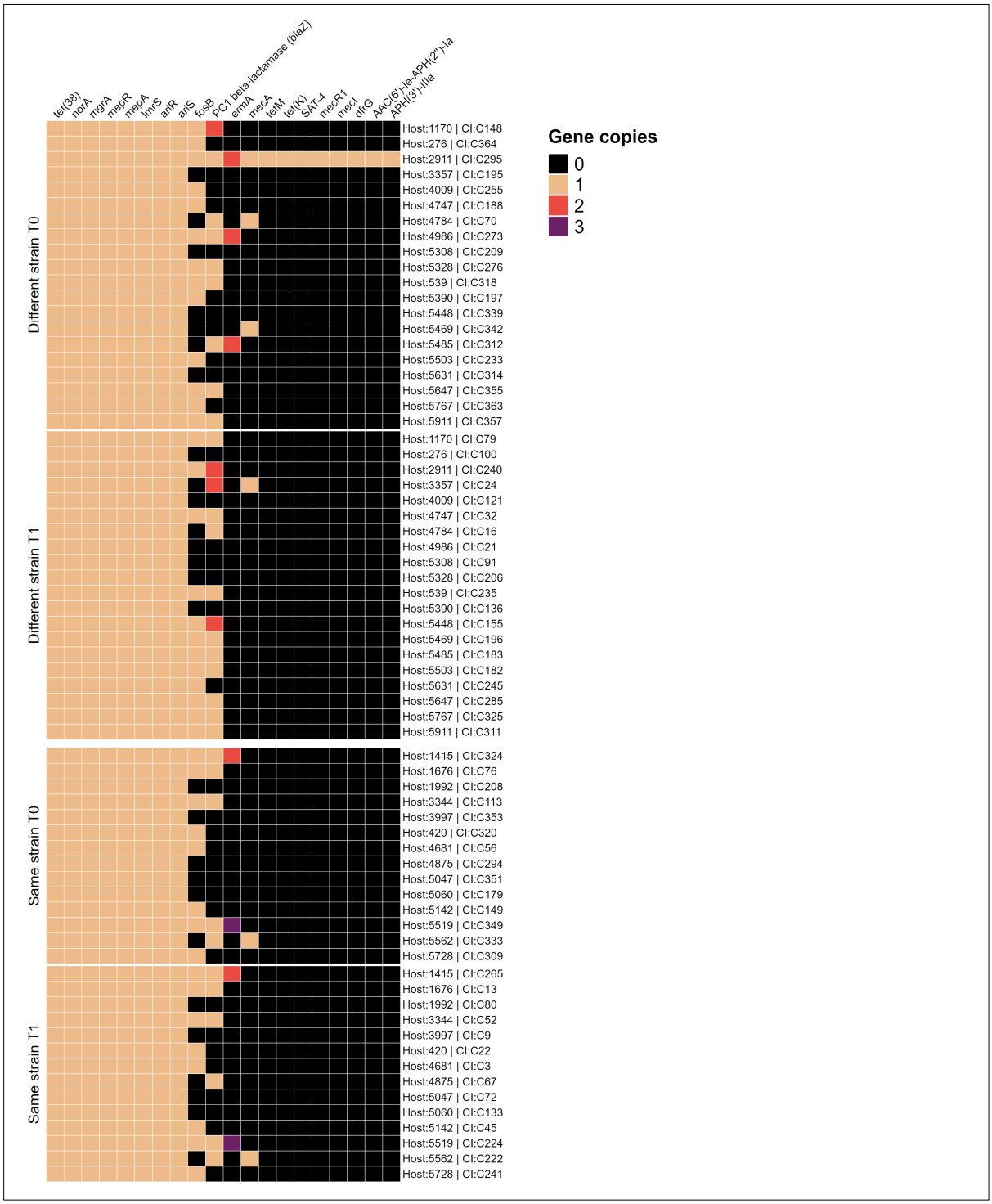

967

968 Figure S1. Gene copy matrix of antimicrobial resistance genes in the genomes of all *S.*

969 *aureus* clinical isolates (n=68). The isolates are represented by the rows and grouped by

970 strain-relatedness classification and the order of CI collection. The gene copies of

971 antimicrobial resistance genes are indicated by colour.

Figure S2

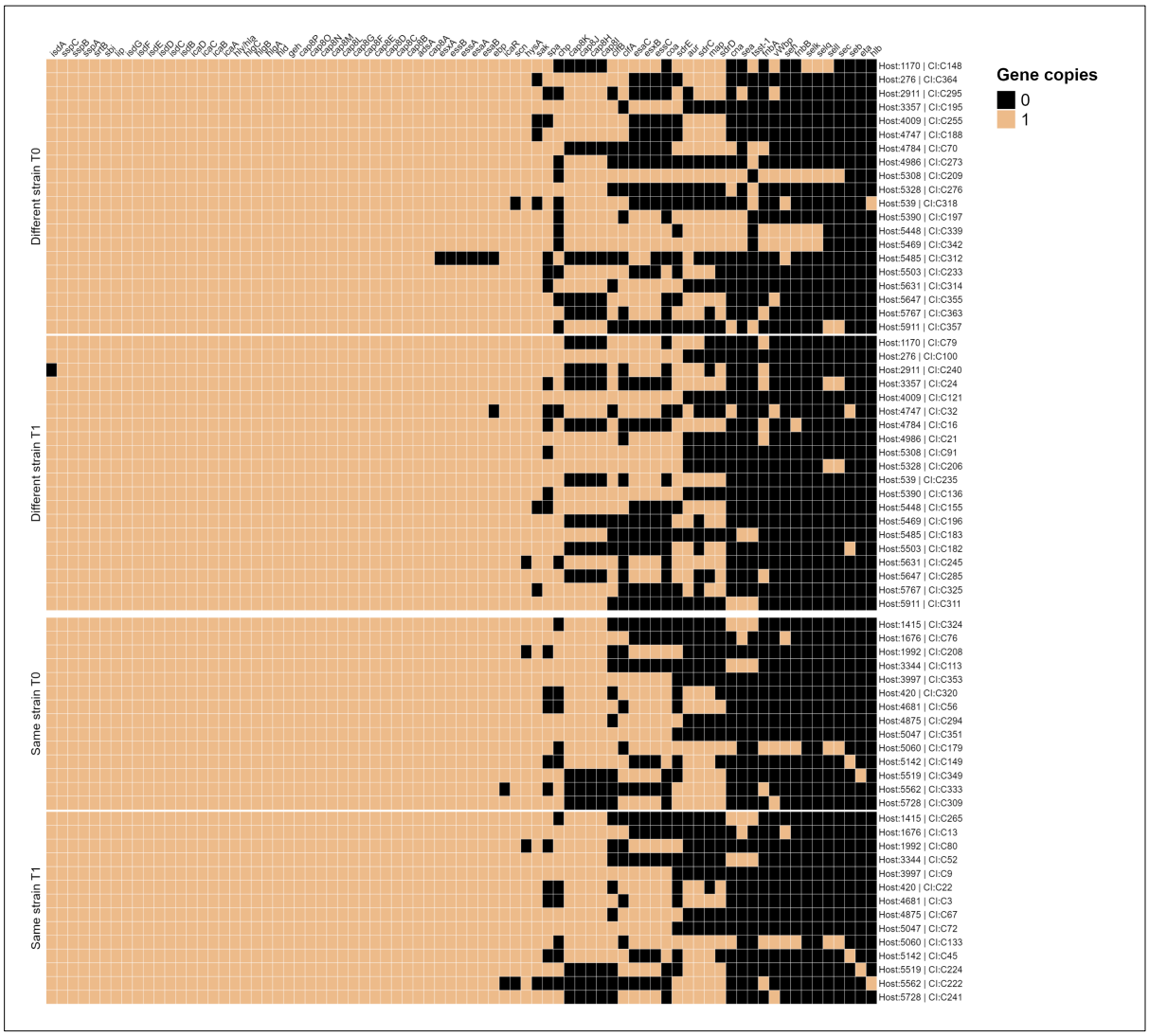

Figure S2. Matrix displaying the virulence genes in the genome of all CIs (n=68). CIs are grouped by strain relatedness and the collection sequence. The matrix is split into strains classified as 'same strain' pairs (N=14) and 'different strain' pairs (N=20). T0 and T1 indicate the first and second CIs groups of the sequential *S. aureus* pairs, respectively.

978 **Figure S3**

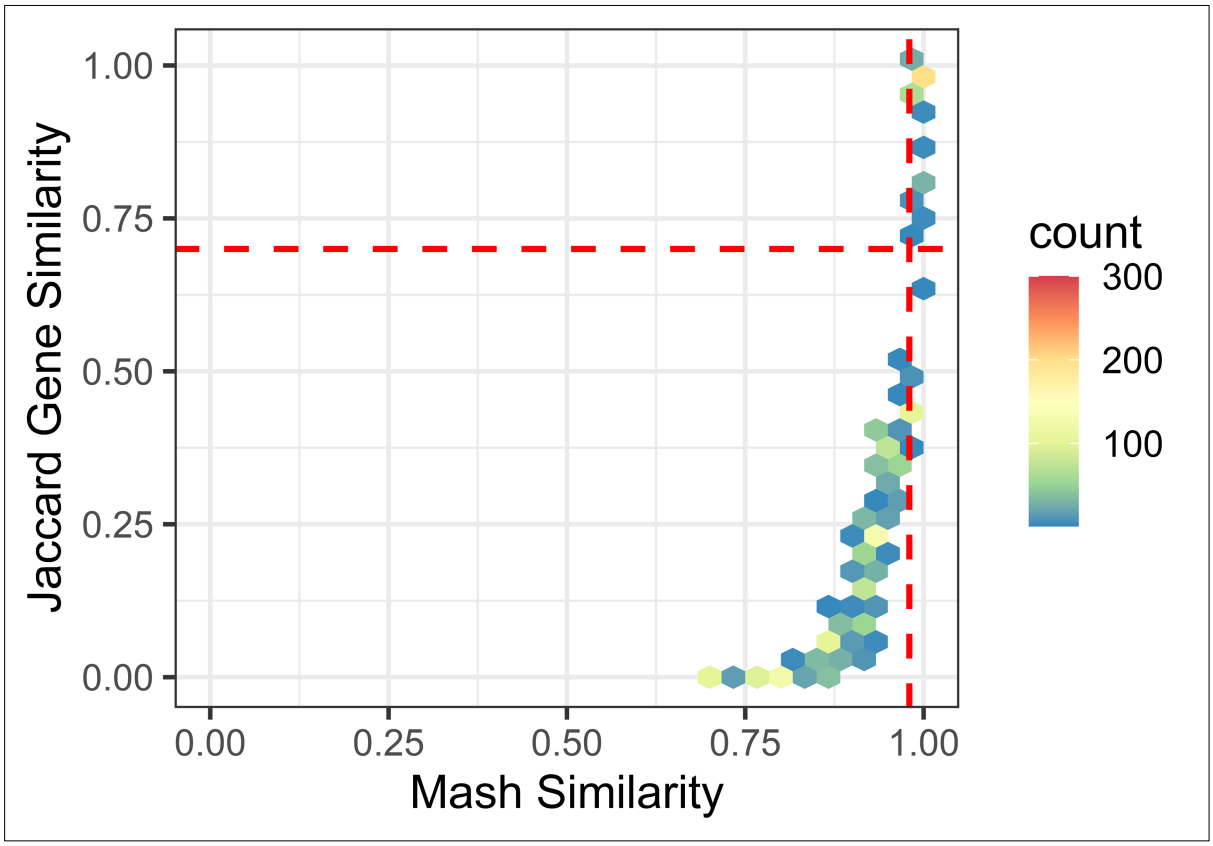

979

980 Figure S3. Hexagonal binned plot displaying the relationship between all the plasmids
981 detected based on gene presence and absence and M similarity (n=2,756). The
982 hexagonal cell colour represents the number of data points observed in that cell.
983 Plasmids were considered the same using a threshold of Mash similarity distance
984 greater than 0.98 and Jaccard index of gene presence and absence greater than 0.7.

985 Figure S4

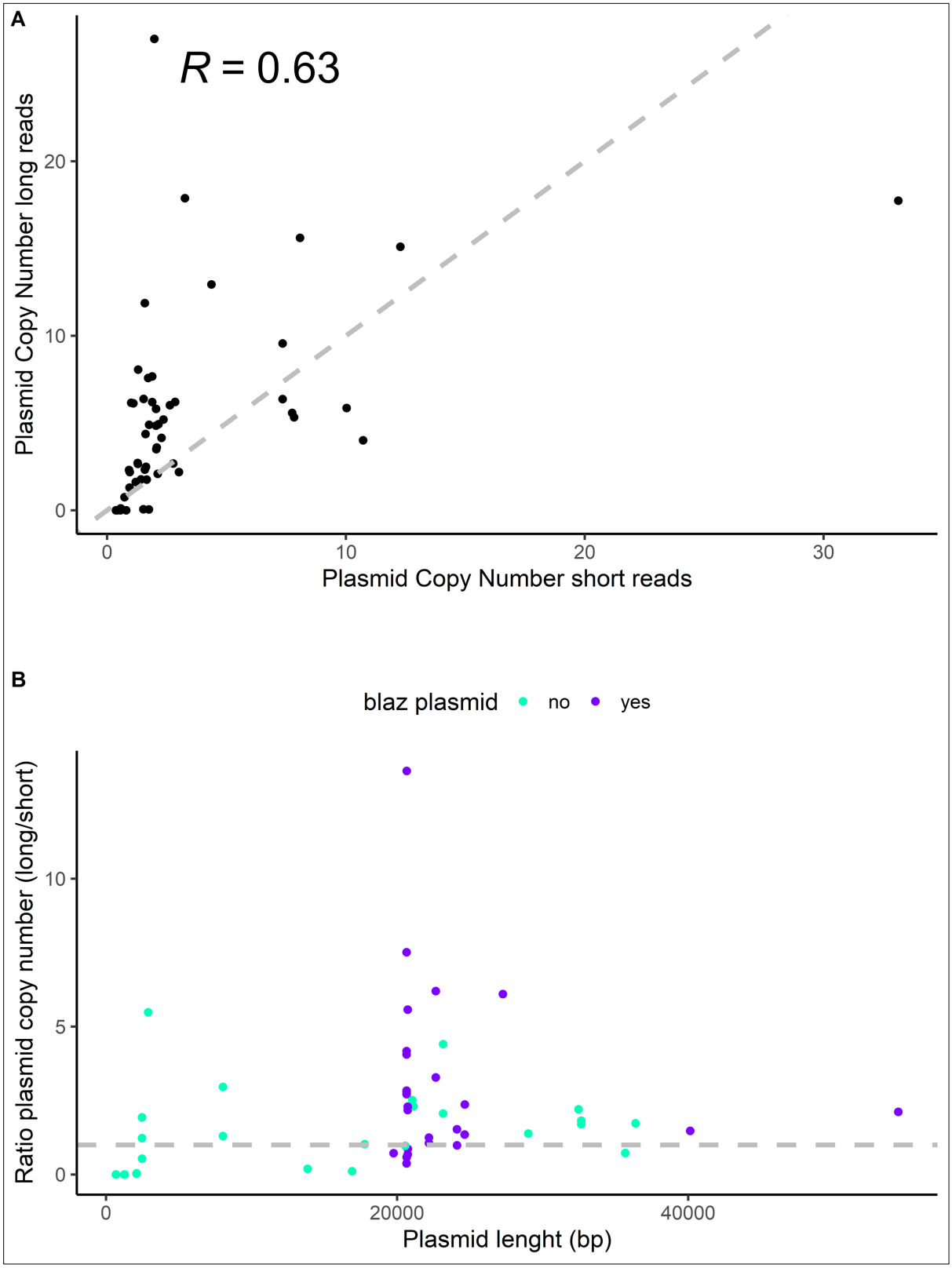

986

987 Figure S4. Comparison of plasmid copy numbers estimated from long-read sequencing

988 versus short-read sequencing. (A) Each point represents a single plasmid (n=53), with

989 the x-axis indicating the copy number from short-read sequencing and the y-axis
990 indicating the copy number from long-read sequencing. The Spearman correlation
991 coefficient is shown in the top left. (B) The ratio of the plasmid copy number
992 (short/long) for all plasmids detected (N=53). *Blaz*-positive plasmids are indicated by
993 colour. The grey line is the intercept of the ratio=1.

994 **Figure S5**

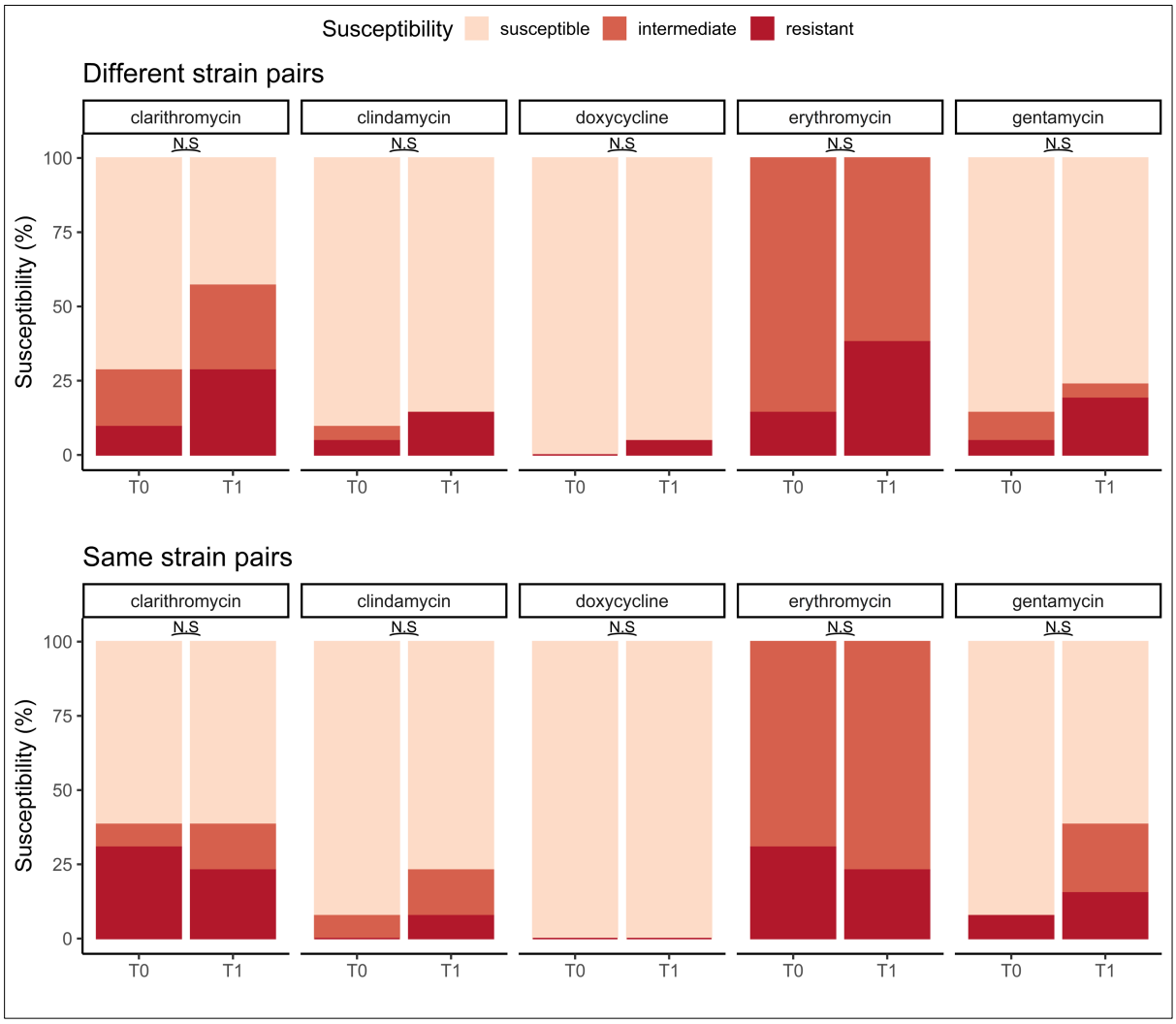

995

996 Figure S5. Planktonic antibiotic susceptibility of *S. aureus* isolates (n=68). Antibiotic
997 susceptibility of *S. aureus* isolates is presented based on minimum inhibitory
998 concentration (MIC) breakpoints adapted from the CLSI for isolates classified as the
999 same and different strains (N=14, N=20). Fisher's exact test was used to determine the
1000 significant difference in the proportion of resistant and non-resistant isolates between
1001 the T0 and T1 groups, with a threshold of $p<0.05$. MIC breakpoints are not available for
1002 augmentin and mupirocin.

1003 **Figure S6**

1004
1005 Figure S6. Swimmer plot showing the timeline of antibiotic prescription for each subject

1006 between the collection of the first and second timepoint isolates. The antibiotics are

1007 indicated by colour. The top green bar represents the time between isolate collection.

1008 The left column represents all 'same strain' isolates, and the right column represents

1009 'different strain' isolates. Host ID numbers are indicated on the right side of the columns.

Figure S7

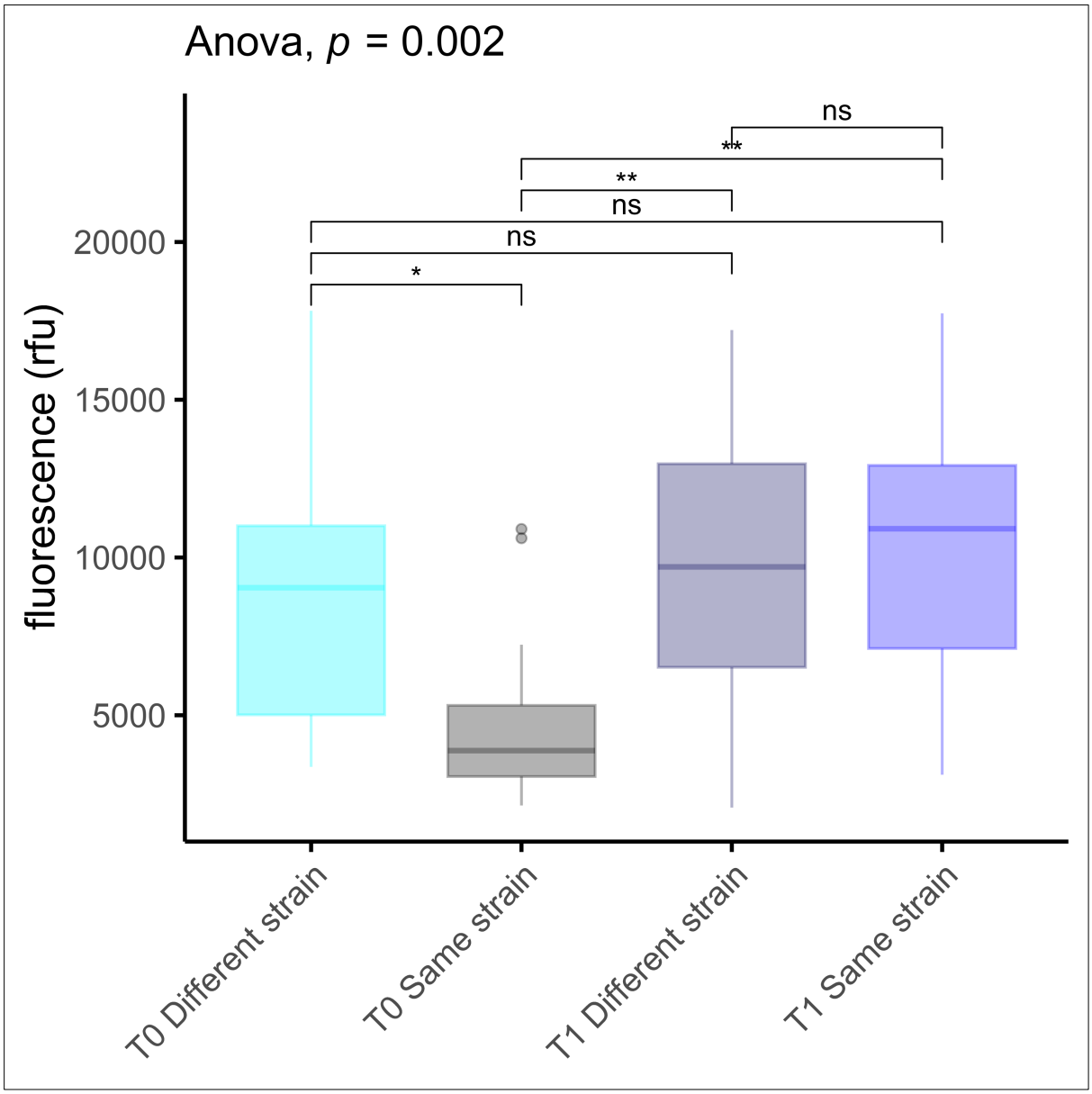

Figure S7. *S. aureus* biofilms viability after 48 hours of growth for all 68 clinical isolates (CIs). The x-axis indicates the first and second CIs classified as the 'same strain' and 'different strain'. Significance was tested using ANOVA, and post-hoc pairwise t-test with Bonferroni correction applied for multiple comparisons.

Supplementary text

ST1

Chronic rhinosinusitis (CRS) diagnosis criteria as described by the EPOS:

The presence of two or more symptoms, one of which should be either nasal blockage or nasal discharge with facial pain/pressure or loss of smell. The symptoms should last for more than 12 weeks. Patients were considered difficult-to-treat if no acceptable level of control was achieved despite adequate surgery, intranasal corticosteroid treatment and short courses of antibiotics or systemic corticosteroids in the preceding year of collection.

Asthma status and aspirin sensitivity were collected via self-reported questionnaires at the time of consent for the biobank. Furthermore, an ENT surgeon added the CRS subtype to the biobank after endoscopic assessment.

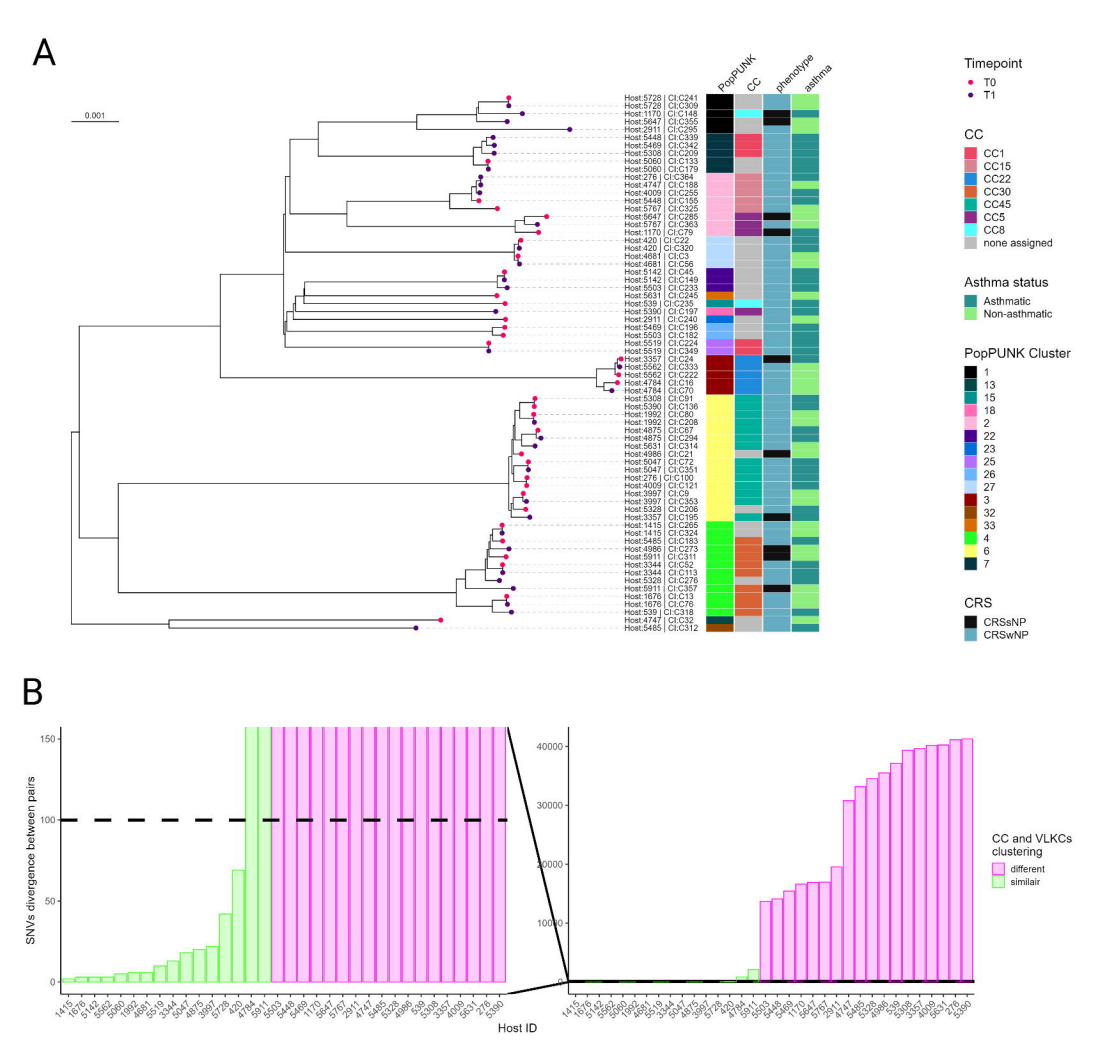
A
0.001
PopPUNK
CC
phenotype
asthma
Timepoint
T0
T1
CC
CC1
CC15
CC22
CC30
CC45
CC5
CC8
none assigned
Asthma status
Asthmatic
Non-asthmatic
PopPUNK Cluster
1
13
15
18
2
22
23
25
26
27
3
32
33
4
6
7
CRS
CRSsNP
CRSwNP
B
SNVs divergence between pairs
Host ID
CC and VLKCs clustering
different
similair

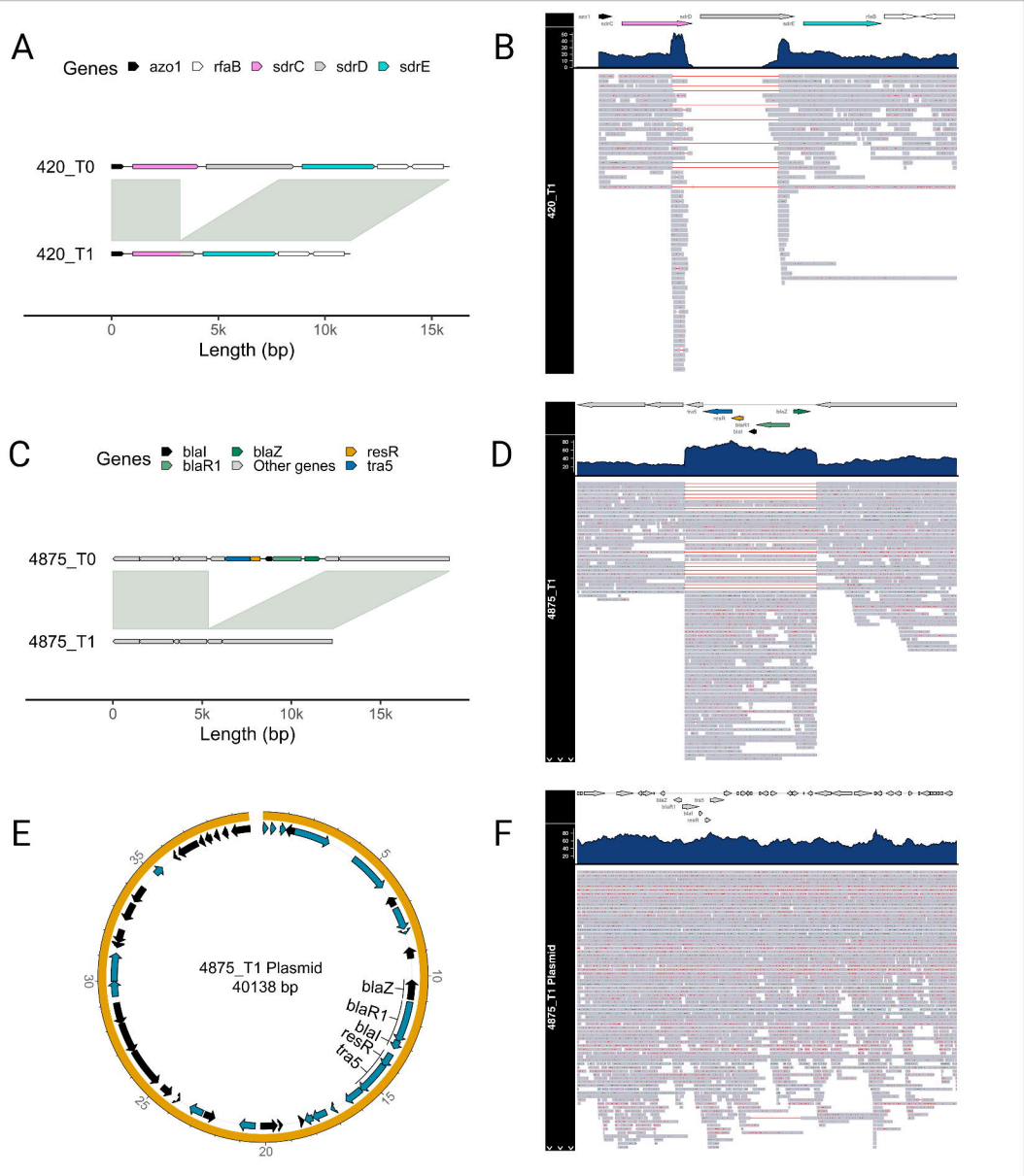
A
Genes azo1 rfaB sdrC sdrD sdrE
420_T0
420_T1
0
5k
10k
15k
Length (bp)
B
420_T1
C
Genes blaI blaR1 blaZ Other genes resR tra5
4875_T0
4875_T1
0
5k
10k
15k
Length (bp)
D
4875_T1
E
4875_T1 Plasmid
40138 bp
blaZ
blaR1
blaI
resR
tra5
F
4875_T1 Plasmid

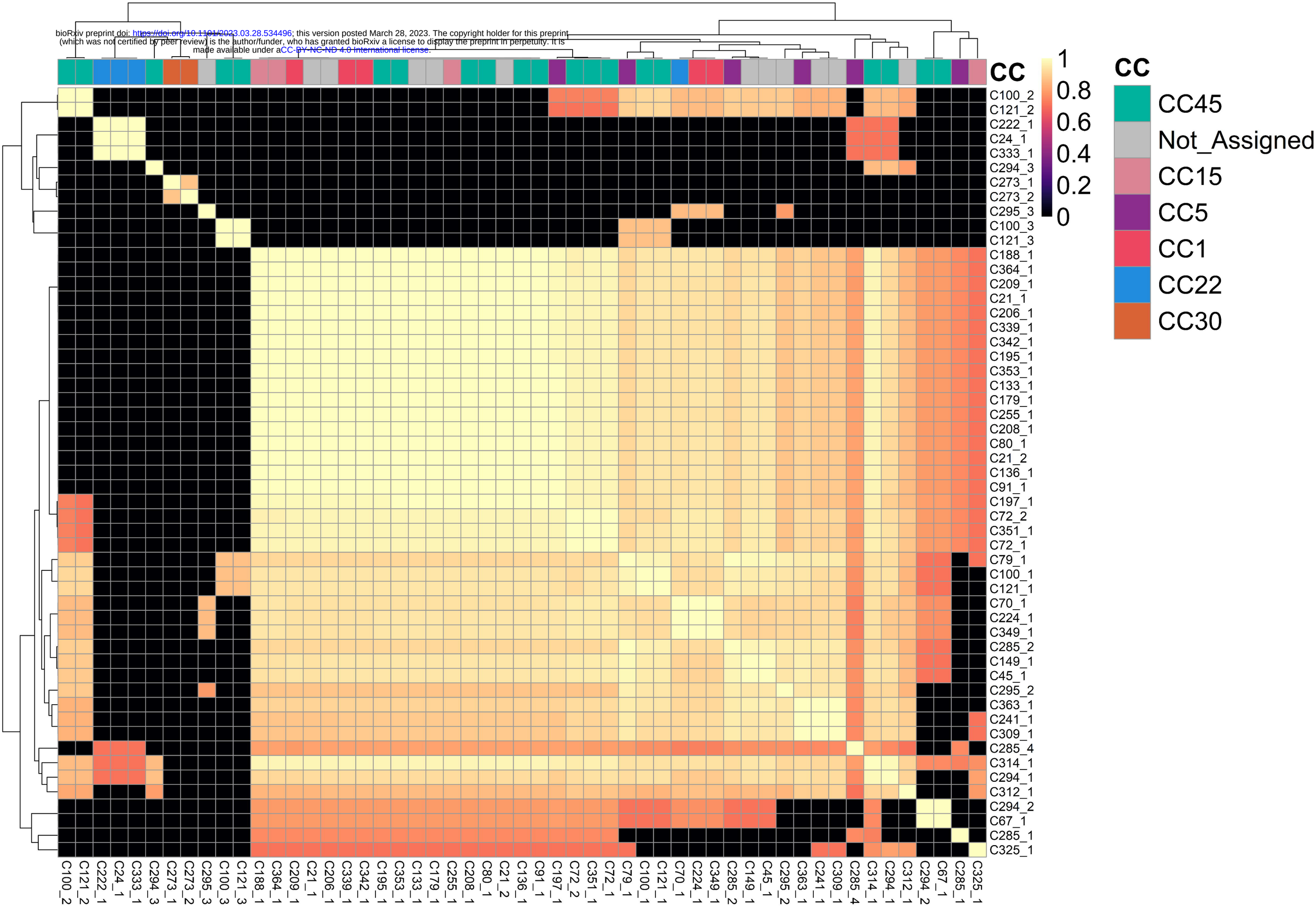

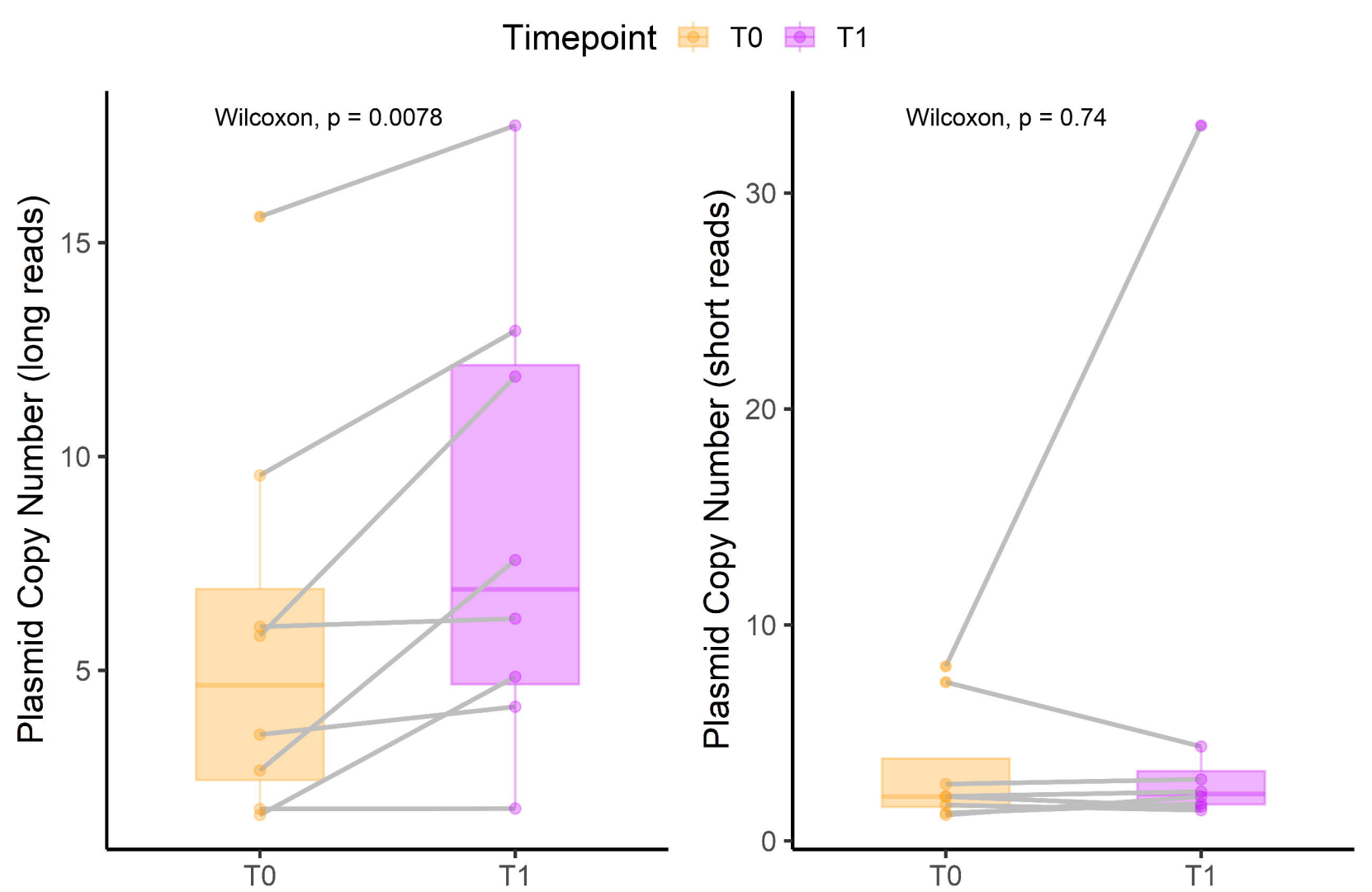
Timepoint
T0
T1
Wilcoxon, p = 0.0078
Plasmid Copy Number (long reads)
15
10
5
T0
T1
Wilcoxon, p = 0.74
Plasmid Copy Number (short reads)
30
20
10
0
T0
T1

A

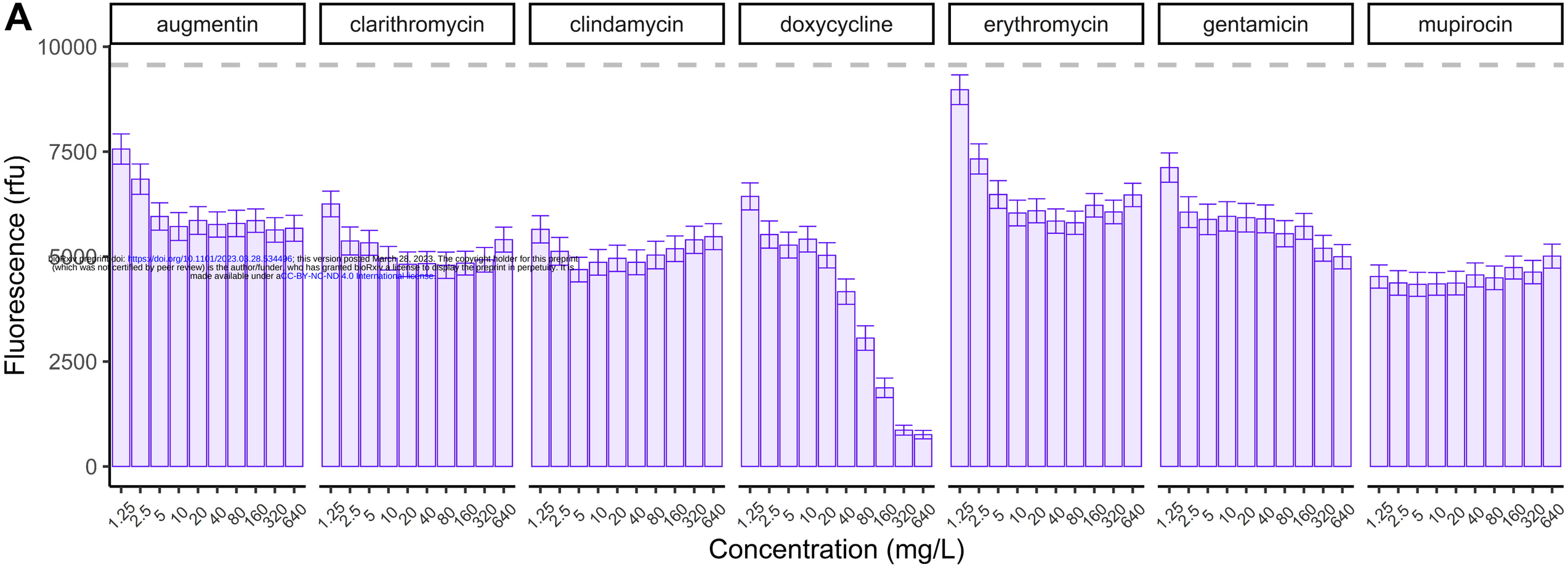

B

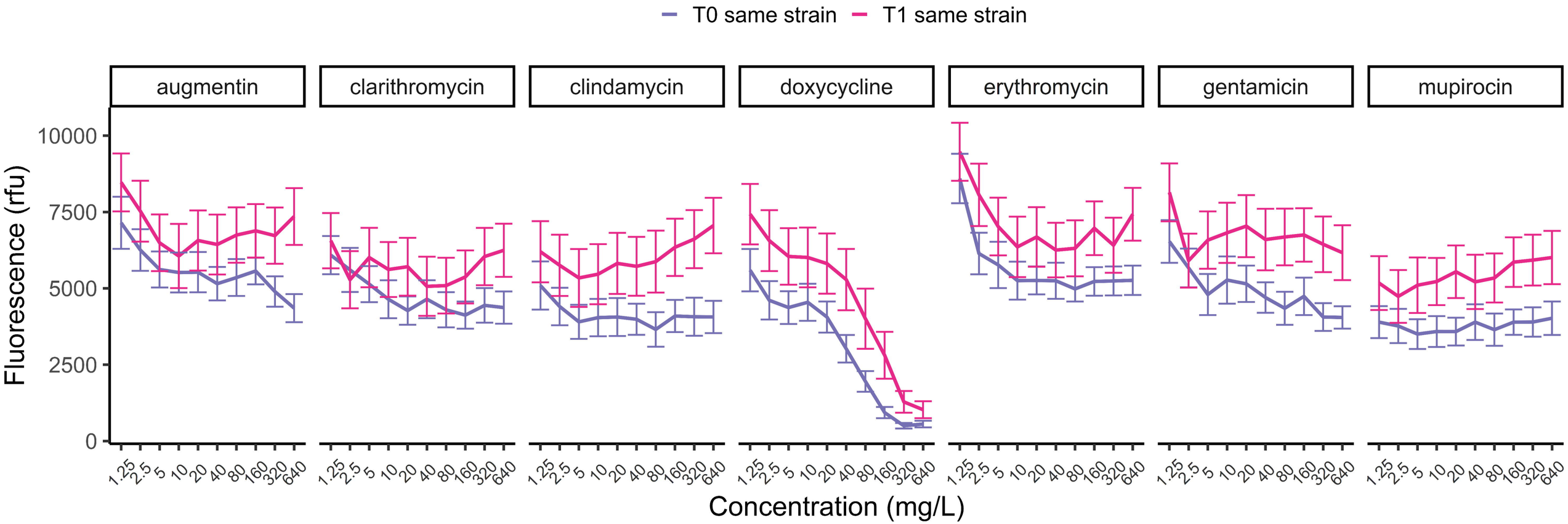

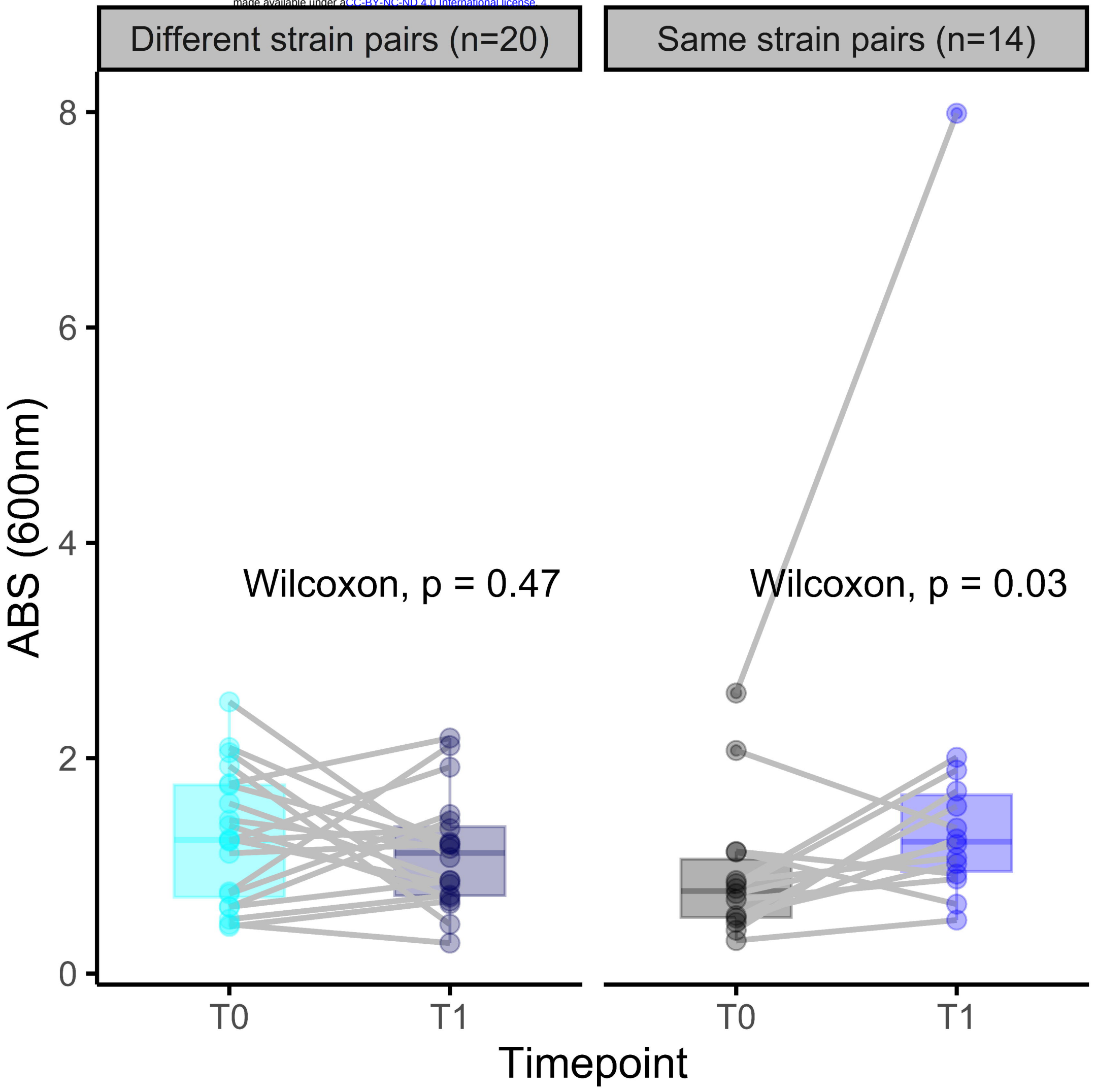

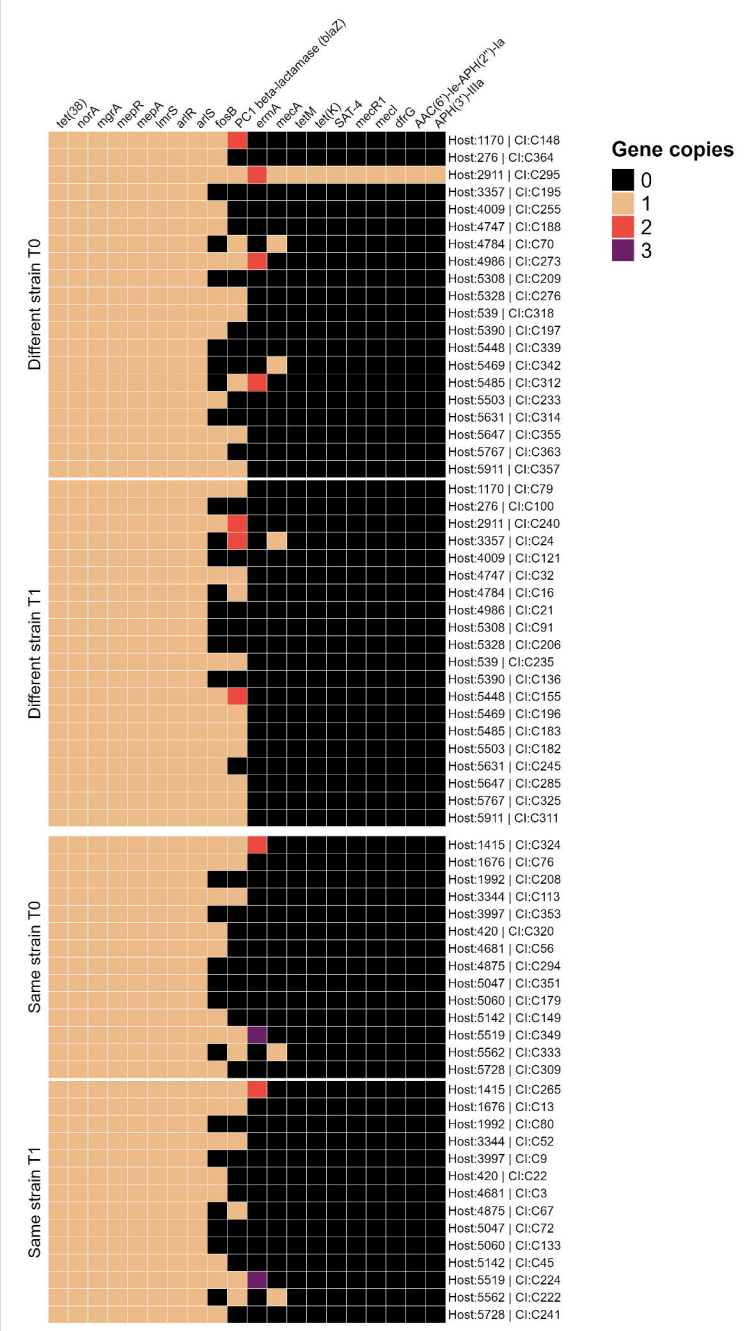
tet(38)
norA
mgrA
mepR
mepA
lmrS
arlR
arlS
fosB
PC1 beta-lactamase (blaZ)
ermA
mecA
tetM
tet(K)
SAT-4
mecR1
mecI
dfrG
AAC(6')-Ie-APH(2")-Ia
APH(3')-IIIa
Gene copies
0
1
2
3
Different strain T0
Host:1170 | Cl:C148
Host:276 | Cl:C364
Host:2911 | Cl:C295
Host:3357 | Cl:C195
Host:4009 | Cl:C255
Host:4747 | Cl:C188
Host:4784 | Cl:C70
Host:4986 | Cl:C273
Host:5308 | Cl:C209
Host:5328 | Cl:C276
Host:539 | Cl:C318
Host:5390 | Cl:C197
Host:5448 | Cl:C339
Host:5469 | Cl:C342
Host:5485 | Cl:C312
Host:5503 | Cl:C233
Host:5631 | Cl:C314
Host:5647 | Cl:C355
Host:5767 | Cl:C363
Host:5911 | Cl:C357
Different strain T1
Host:1170 | Cl:C79
Host:276 | Cl:C100
Host:2911 | Cl:C240
Host:3357 | Cl:C24
Host:4009 | Cl:C121
Host:4747 | Cl:C32
Host:4784 | Cl:C16
Host:4986 | Cl:C21
Host:5308 | Cl:C91
Host:5328 | Cl:C206
Host:539 | Cl:C235
Host:5390 | Cl:C136
Host:5448 | Cl:C155
Host:5469 | Cl:C196
Host:5485 | Cl:C183
Host:5503 | Cl:C182
Host:5631 | Cl:C245
Host:5647 | Cl:C285
Host:5767 | Cl:C325
Host:5911 | Cl:C311
Same strain T0
Host:1415 | Cl:C324
Host:1676 | Cl:C76
Host:1992 | Cl:C208
Host:3344 | Cl:C113
Host:3997 | Cl:C353
Host:420 | Cl:C320
Host:4681 | Cl:C56
Host:4875 | Cl:C294
Host:5047 | Cl:C351
Host:5060 | Cl:C179
Host:5142 | Cl:C149
Host:5519 | Cl:C349
Host:5562 | Cl:C333
Host:5728 | Cl:C309
Same strain T1
Host:1415 | Cl:C265
Host:1676 | Cl:C13
Host:1992 | Cl:C80
Host:3344 | Cl:C52
Host:3997 | Cl:C9
Host:420 | Cl:C22
Host:4681 | Cl:C3
Host:4875 | Cl:C67
Host:5047 | Cl:C72
Host:5060 | Cl:C133
Host:5142 | Cl:C45
Host:5519 | Cl:C224
Host:5562 | Cl:C222
Host:5728 | Cl:C241

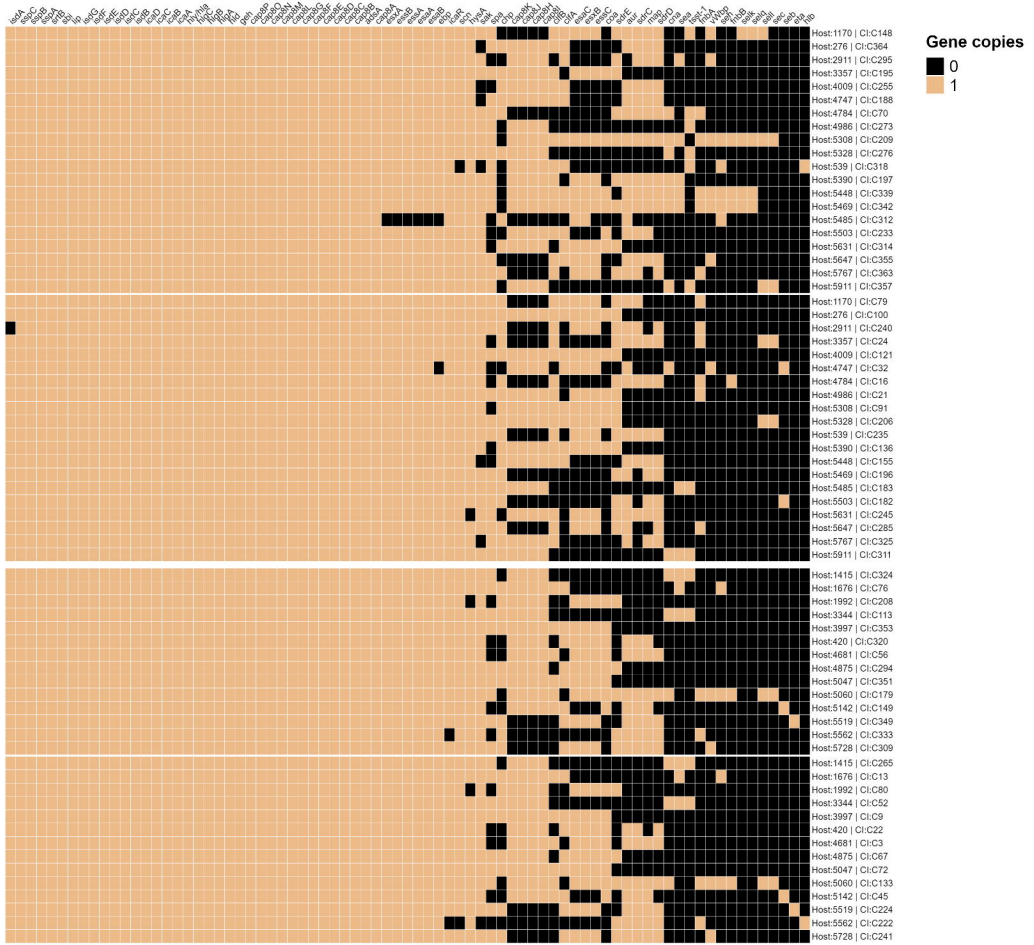
Gene copies
0
1
Different strain T0
Different strain T1
Same strain T0
Same strain T1
Host:1170 | Cl:C148
Host:276 | Cl:C364
Host:2911 | Cl:C295
Host:3357 | Cl:C195
Host:4009 | Cl:C255
Host:4747 | Cl:C188
Host:4784 | Cl:C70
Host:4986 | Cl:C273
Host:5308 | Cl:C209
Host:5328 | Cl:C276
Host:539 | Cl:C318
Host:5390 | Cl:C197
Host:5448 | Cl:C339
Host:5469 | Cl:C342
Host:5485 | Cl:C312
Host:5503 | Cl:C233
Host:5631 | Cl:C314
Host:5647 | Cl:C355
Host:5767 | Cl:C363
Host:5911 | Cl:C357
Host:1170 | Cl:C79
Host:276 | Cl:C100
Host:2911 | Cl:C240
Host:3357 | Cl:C24
Host:4009 | Cl:C121
Host:4747 | Cl:C32
Host:4784 | Cl:C16
Host:4986 | Cl:C21
Host:5308 | Cl:C91
Host:5328 | Cl:C206
Host:539 | Cl:C235
Host:5390 | Cl:C136
Host:5448 | Cl:C155
Host:5469 | Cl:C196
Host:5485 | Cl:C183
Host:5503 | Cl:C182
Host:5631 | Cl:C245
Host:5647 | Cl:C285
Host:5767 | Cl:C325
Host:5911 | Cl:C311
Host:1415 | Cl:C324
Host:1676 | Cl:C76
Host:1992 | Cl:C208
Host:3344 | Cl:C113
Host:3997 | Cl:C353
Host:420 | Cl:C320
Host:4681 | Cl:C56
Host:4875 | Cl:C294
Host:5047 | Cl:C351
Host:5060 | Cl:C179
Host:5142 | Cl:C149
Host:5519 | Cl:C349
Host:5562 | Cl:C333
Host:5728 | Cl:C309
Host:1415 | Cl:C265
Host:1676 | Cl:C13
Host:1992 | Cl:C80
Host:3344 | Cl:C52
Host:3997 | Cl:C9
Host:420 | Cl:C22
Host:4681 | Cl:C3
Host:4875 | Cl:C67
Host:5047 | Cl:C72
Host:5060 | Cl:C133
Host:5142 | Cl:C45
Host:5519 | Cl:C224
Host:5562 | Cl:C222
Host:5728 | Cl:C241

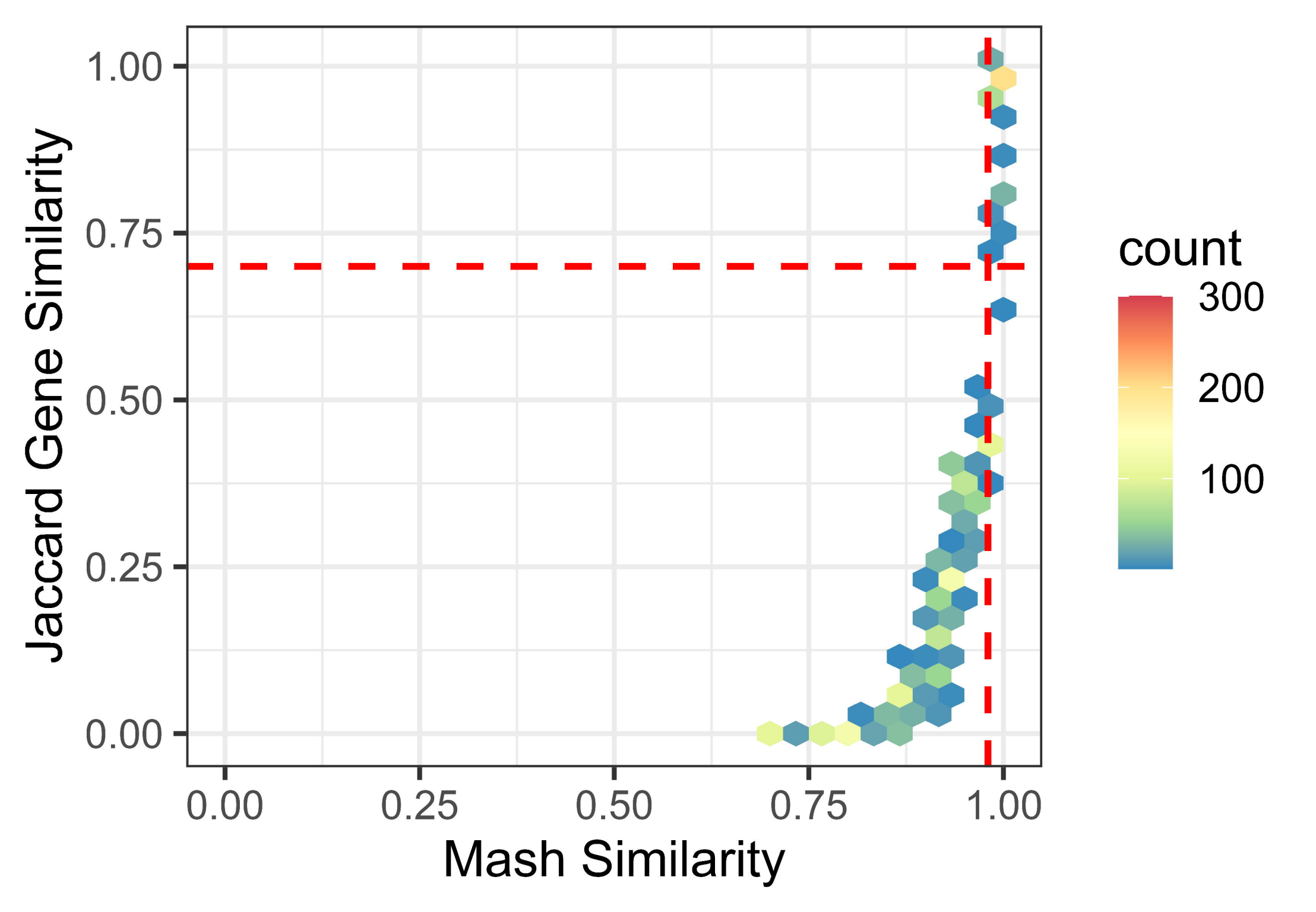
Jaccard Gene Similarity
1.00
0.75
0.50
0.25
0.00
0.00
0.25
0.50
0.75
1.00
Mash Similarity
count
300
200
100

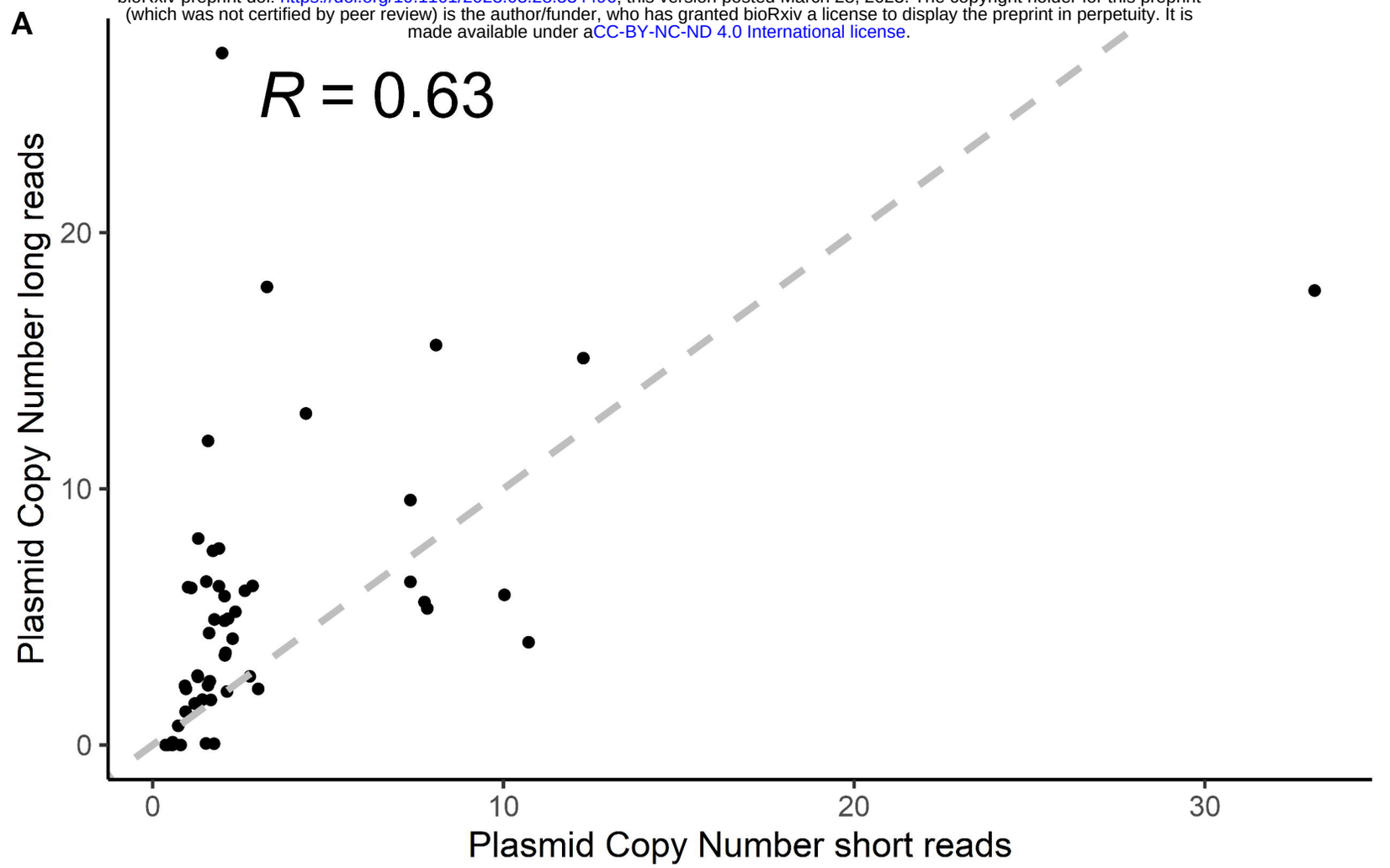

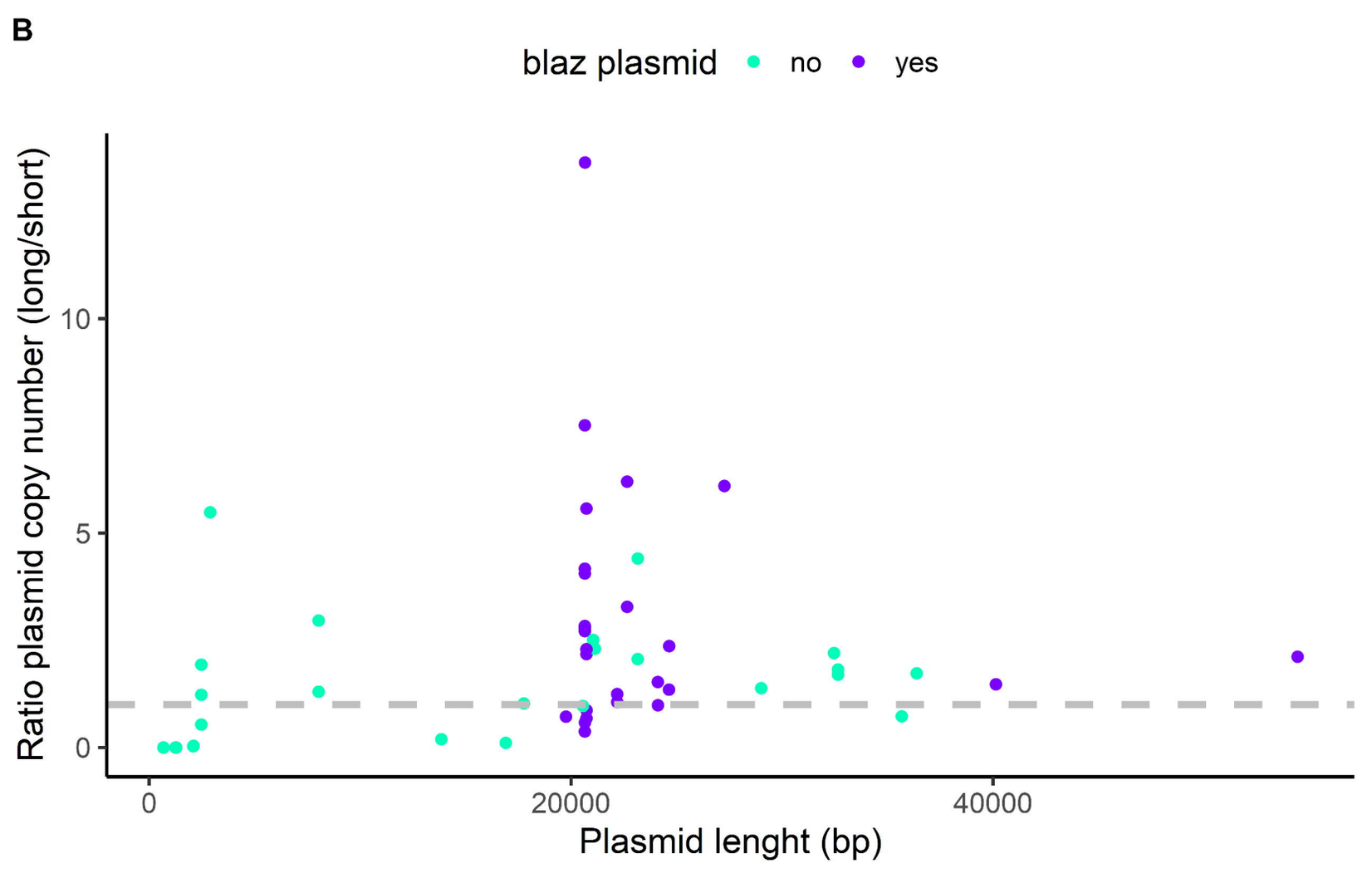

Susceptibility susceptible intermediate resistant

Different strain pairs

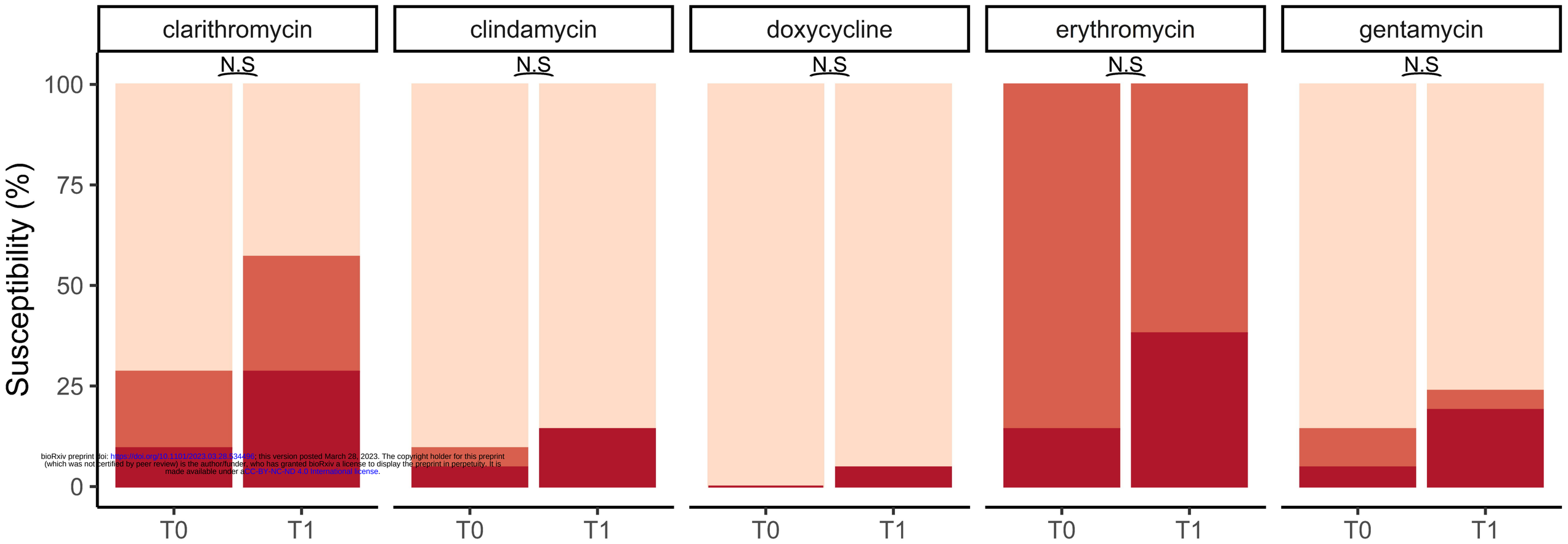

Same strain pairs

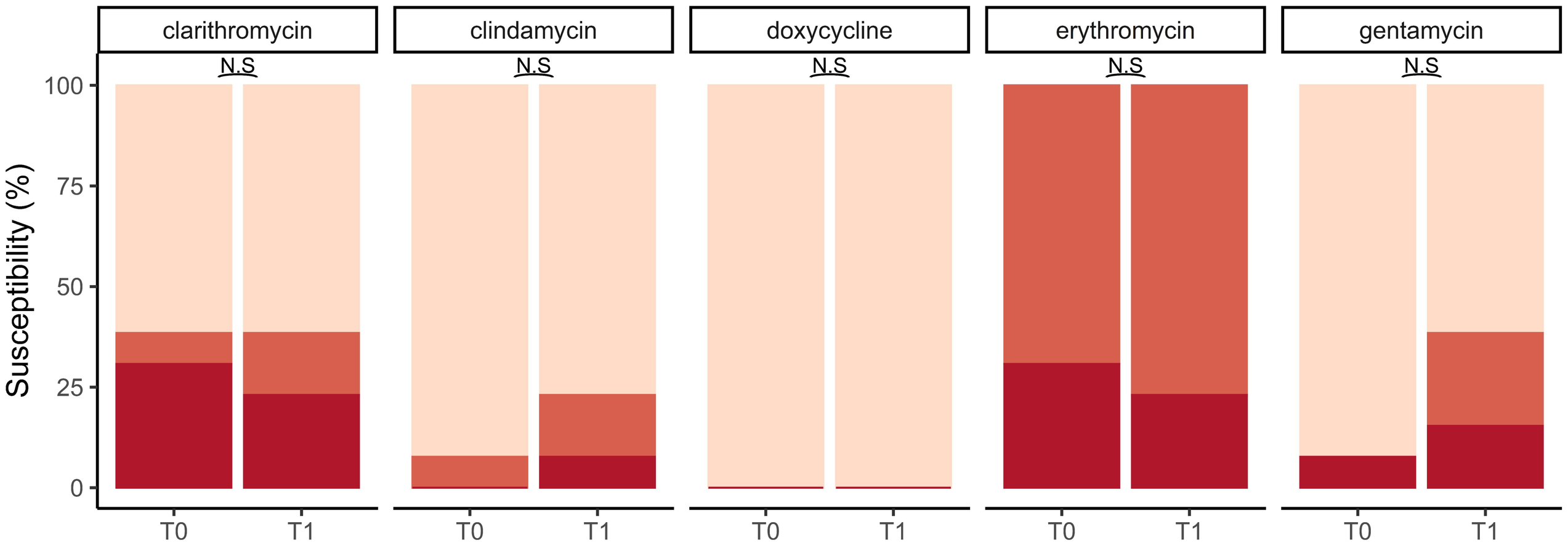


Augmentin
Ciprofloxacin 500mg
mupirocin 0.05% Nasal rinse
Tobramycin Nasal rinse
Trimethoprim/Sulfamethoxazole
Doxycycline 50mg
Clarithromycin 250mg
Clindamycin 150mg
Doxycycline 100mg
Moxifloxacin 400mg
Follow-up
Same strain CIs
1415
1676
1992
3344
3997
420
4681
4875
5047
5060
5142
5519
5562
5728
0
500
1000
1500
Time (days)
Different strain CIs
1170
276
2811
3357
4009
4747
4784
4986
5308
5328
539
5390
5448
5469
5485
5503
5631
5647
5767
5911
0
500
1000
Time (days)